

# Skin Cancer Detection and Classification Using Multiple Optimized Deep Convolutional Neural Network

by

Adnan Sakir (18101669)  
Mustakim Anwar Chowdhury (18101591)  
Maksura Rahman(18101068)  
K. M Shefat Mostafiz (18101619)

A thesis submitted to the Department of Computer Science and Engineering  
in partial fulfillment of the requirements for the degree of  
B.Sc. in Computer Science and Engineering

Department of Computer Science and Engineering  
BRAC University  
May, 2022

© 2022. Brac University  
All rights reserved.

# Declaration

It is hereby declared that

1. The thesis submitted is my/our own original work while completing degree at BRAC University.
2. The thesis does not contain material previously published or written by a third party, except where this is appropriately cited through full and accurate referencing.
3. The thesis does not contain material which has been accepted, or submitted, for any other degree or diploma at a university or other institution.
4. We have acknowledged all main sources of help.

**Student's Full Name & Signature:**

---

Adnan Sakir  
18101669

---

Mustakim Anwar Chowdhury  
18101591

---

Maksura Rahman  
18101068

---

K. M Shefat Mostafiz  
18101619

# Approval

The thesis titled “Skin Cancer Detection and Classification Using Multiple Optimized Deep Convolutional Neural Network” submitted by

1. Adnan Sakir (18101669)
2. Mustakim Anwar Chowdhury (18101591)
3. Maksura Rahman (18101068)
4. K. M Shefat Mostafiz (18101619)

Of Spring, 2022 has been accepted as satisfactory in partial fulfillment of the requirement for the degree of B.Sc. in Computer Science and Engineering on May 29, 2022.

## Examining Committee:

Supervisor and Program Coordinator:  
(Member)

---

Annajiat Alim Rasel  
Senior Lecturer  
Department of Computer Science and Engineering  
BRAC University

Co-Supervisor:  
(Member)

---

Moin Mostakim  
Lecturer  
Department of Computer Science and Engineering  
BRAC University

Thesis Coordinator:  
(Member)

---

Md. Golam Rabiul Alam, PhD  
Associate Professor  
Department of Computer Science and Engineering  
BRAC University

Departmental Head:  
(Chair)

---

Sadia Hamid Kazi  
Chairperson and Associate Professor  
Department of Computer Science and Engineering  
Brac University

# Abstract

This work tries to detect skin cancer and classify its type using datasets containing labeled images and classes, using pre-trained CNN models and merged pre-trained CNN models. Skin cancer is an abnormal growth of skin cells that most usually occurs on sun-exposed skin, although it can also develop in areas of your skin that are not normally exposed to sunlight. Skin cancer is a kind of malignant melanoma, which is a type of cancer. Melanoma, basal cell carcinoma, and squamous cell carcinoma are the three types of skin cancer that are diagnosed most frequently. According to projections made by the American Cancer Society (ACS), the number of newly diagnosed cases of melanoma in the United States would reach around 99,780 in the year 2022. (about 57,180 in men and 42,600 in women). It has been estimated that around 7,650 persons are at danger of passing away as a direct result of melanoma (about 5,080 men and 2,570 women). In 2022, the United States expected to see 99,780 new cases of melanoma, 101,280 non-invasive (in situ) cases, and 106,110 invasive cases. Bangladesh is at 183 in the world rank. Skin cancer claims the lives of about 301 persons each year. Basal cell carcinoma is the most common type of skin cancer (also known as basal cell skin cancer). More than 80 percent of all cases of skin cancer are caused by basal cell carcinomas. The basal cell layer, which is located in the lowest section of the epidermis, is where these cancers start. It will be quite difficult to attain high accuracy if you rely just on the dataset that was received from Kaggle. Take into consideration that not all datasets are balanced.

This paper therefore focuses on finding different techniques to achieve the most accuracy on both large and small datasets with the help of Deep CNN models such as VGG19, VGG16, ResNet50, InceptionV3 and combining two deep CNN models. These techniques primarily rely on supervised learning, which leverages datasets training data points and labels. Here, we have merged various pretrained models such as the VGG19, VGG16, ResNet50 and InceptionV3 and have passed it into our CNN model. Moreover, we have used image inputs as 224 x 224 pixels. Furthermore we have used Keras pre-process input applications with the help of image data generator. Skin cancers images illustrate variations in different characteristics. Evaluation of the results of the segmentation algorithm can be equally complex. There will be a calculator that calculates the percentage of loss. There is possibly various clinical attributes that points out the skin cancer and classify its type.

**Keywords:** Transfer Learning, Convolution Neural Network; Cancer detection; Image Classification; Machine Learning Algorithms; Deep Learning.

## **Dedication**

This paper is dedicated to my institution mentors under whose constant guidance I have completed this dissertation. They not only enlightened me with academic knowledge but also gave me valuable advice whenever I needed it the most.

## Acknowledgement

A journey is simpler when traveled with greater vigor. Interdependence is certainly more valuable than independence. The real spirit of achieving a goal is through the way of excellence and perpetual discipline. I would have never succeeded in completing my task without the cooperation, encouragement and help provided to me by various personalities.

First of all, I render my gratitude to the almighty who bestowed self-confidence, ability and strength in me to complete this work. Without his grace this would have never been a reality.

With deep sense of gratitude I express my sincere thanks to my esteemed and worthy Supervisor Mr. ANNAJIAT ALIM RASEL, Senior Lecturer, Department of Computer Science and Engineering for his valuable guidance in carrying out this work under his effective supervision, encouragement, enlightenment and cooperation.

I am grateful to our Co-Supervisor Mr. MOIN MOSTAKIM, Lecturer, Department of Computer Science and Engineering for his constant support and encouragement that was of great importance in the completion of this thesis. I am also thankful to all the staff members of the department for their full cooperation and help.

My greatest thanks to all who wished me success, especially my parents and friends whose support and care made me stay on earth.

# Table of Contents

Cover	i
Declaration	i
Approval	ii
Abstract	iv
Dedication	v
Acknowledgement	vi
Table of Contents	vii
List of Tables	ix
Nomenclature	x
Thesis Structure	xi
<b>1 Introduction</b>	<b>1</b>
1.1 Motivation . . . . .	3
1.2 Research Problem . . . . .	3
1.3 Research Objective . . . . .	5
<b>2 Literature Review</b>	<b>7</b>
2.1 Related Work . . . . .	11
2.2 Seven Types of Skin Cancer . . . . .	13
2.2.1 Actinic Keratosis and Intraepithelial Carcinoma . . . . .	13
2.2.2 Basal Cell Carcinoma . . . . .	15
2.2.3 Benign Keratosis-like Lesions . . . . .	16
2.2.4 Dermatofibroma . . . . .	17
2.2.5 Melanoma . . . . .	17
2.2.6 Melanocytic Nevi . . . . .	18
2.2.7 Vascular Lesions . . . . .	19
<b>3 Data Description</b>	<b>21</b>
3.1 Dataset Background . . . . .	21
3.2 Dataset Classification . . . . .	22
3.3 Dataset Sources and Comparisons . . . . .	24



3.3.1	Rosendahl Image Set . . . . .	24
3.3.2	ViDIR Group . . . . .	24
3.4	Technical Validation . . . . .	25
<b>4</b>	<b>Dataset</b>	<b>26</b>
4.1	Required Libraries . . . . .	26
4.2	Data Cleaning . . . . .	26
4.3	Exploratory Data Analysis . . . . .	26
4.3.1	Distribution of Type of Cancer . . . . .	27
4.3.2	Distribution with Diagnosis Type . . . . .	27
4.3.3	Distribution with Localization . . . . .	28
4.3.4	Distribution with Gender . . . . .	29
4.3.5	Distribution with Age . . . . .	29
4.3.6	Scatter-plot Diagram of Distribution of Age Against Dis- tribution of Cancer . . . . .	30
<b>5</b>	<b>Data Augmentation</b>	<b>31</b>
5.1	Reading and Processing the Data . . . . .	31
5.1.1	Loading and Resizing . . . . .	32
5.2	Train-Test Split . . . . .	32
5.3	Normalization . . . . .	32
5.3.1	Label-Encoding . . . . .	32
5.3.2	Splitting Training and Validation Split . . . . .	33
<b>6</b>	<b>Model Building</b>	<b>34</b>
6.1	Work Plan . . . . .	34
6.2	Our Model and Initial Iteration . . . . .	36
<b>7</b>	<b>Model Evaluation and Result Analysis</b>	<b>38</b>
7.1	Annealing . . . . .	38
7.2	Fitting Model . . . . .	38
7.3	Transfer Learning Using One Pre-trained Model . . . . .	39
7.3.1	Transfer Learning with VGG-16 . . . . .	39
7.3.2	Transfer Learning with VGG19 . . . . .	40
7.3.3	Transfer Learning with ResNet50 . . . . .	41
7.3.4	Transfer Learning with InceptionV3 . . . . .	42
7.4	Transfer Learning with Merged Models . . . . .	43
7.4.1	Transfer Learning with ResNet50 and VGG19 . . . . .	43
7.4.2	Transfer Learning with ResNet50 and VGG16 . . . . .	44
7.4.3	Transfer Learning with ResNet50 and InceptionV3 . . . . .	45
7.4.4	Transfer Learning with VGG16 and InceptionV3 . . . . .	46
7.4.5	Transfer Learning with VGG19 and InceptionV3 . . . . .	47
7.5	Analysis and Comparison of the Models . . . . .	48
<b>8</b>	<b>Conclusion</b>	<b>49</b>
	<b>Bibliography</b>	<b>53</b>

# List of Tables

1.1	Highest rates of skin cancer according to WCRF . . . . .	4
3.1	Overview of ISIC archive and Class Distribution upto April 2020 .	22
3.2	Comparison of HAM10000 with other datasets containing der- matoscopic images that are openly available. . . . .	24
5.1	Label encoding for 7 categories. . . . .	33
7.1	Results of VGG16 . . . . .	39
7.2	Results of VGG19 . . . . .	40
7.3	Results of ResNet50 . . . . .	41
7.4	Results of InceptionV3 . . . . .	42
7.5	Results of concatenated ResNet50 and VGG19 model . . . . .	43
7.6	Results of concatenated ResNet50 and VGG16 model . . . . .	44
7.7	Results of concatenated ResNet50 and InceptionV3 model . . . . .	45
7.8	Results of concatenated VGG16 and InceptionV3 model . . . . .	46
7.9	Results of concatenated VGG19 and InceptionV3 model . . . . .	47
7.10	Test Accuracy and Loss comparisons of all models . . . . .	48

# Nomenclature

The list below contains symbols & abbreviations used in the paper.

*akiec* Actinic Keratoses and Intraepithelial Carcinoma

*ANN* Artificial Neural Network

*bcc* Basal Cell Carcinoma

*bkl* Benign Keratosis

*CNN* Convolutional Neural Network

*df* Dermatofibroma

*EH* Edge Histogram

*HAM* Humans Against Machine

*LBP* Local Binary Pattern

*mel* Melanoma

*NN* Neural Network

*nv* Melanocytic Nevi

*RGB* Red , Green , Blue

*vasc* Vascular Skin Lesions

*ViDir* Vienna Dermatologic Imaging/Informatics Research

# Thesis Structure

The work of this thesis is oriented into some Chapters.

In chapter 1, we will discuss about the motivation, research objective and problem of our work.

In chapter 2, we will talk about the literature review and some related papers on skin cancer.

Chapter 3, describes about the Data pre-processing .

Chapter 4, is all about Data set

Chapter 5, is about how we augment our data.

Chapter 6, indicates how we build our model.

Chapter 7, is all about Model Evaluation and Result analysis.

Chapter 8, conclude the paper.

# Chapter 1

## Introduction

Cancer is a terminology that is used to describe a collection of diseases that are brought on by abnormal cell development and have the capability of infecting or spreading to other areas of the body. Cancer begins almost entirely in the cell. The first signs of cancer might appear in a single cell or in a very small number of cells. According to the World Health Organization (WHO), it is the greatest cause of mortality in the world, accounting for approximately 10 million fatalities in 2020, which is equivalent to roughly one in six deaths. [30] Research has shown that accurate and timely diagnosis can greatly cut down on the fatality rates associated with cancer. There are times when a high degree of expertise is necessary to make a diagnosis, yet despite this, errors in diagnosis or false negatives are regularly produced. Due to the inherent fallibility of human diagnosis, it is imperative that research be conducted into the development of a computerized diagnostic system that is underpinned by deep learning. Through the utilization of a technique known as deep learning, we demonstrate a system that is able to classify the numerous varieties of skin lesions by making use of digital scans and images. Image preprocessing will be used to trim and crop incoming data (digital pictures) to the required dimensions, as well as de-noise foggy images. This will be done in order to meet the requirements of the project. In addition to modifying and extracting certain features of the collection, our model will also establish a relationship between the various stimuli and the appropriate reactions. The technology will work with more precision than other ways, in addition to being more effective and efficient than other methods.

Sun-exposed skin is more likely to develop skin cancer, which is defined as the uncontrolled growth of skin cells. On the other hand, this common kind of cancer can also grow in areas of your skin that are not often subjected to the effects of light. Melanoma and non-melanoma skin cancers are the two categories that fall under the umbrella term "skin cancer." Melanoma, which was listed as the 19th most frequent disease in a recent survey, was found to be the most prevalent type of cancer, with about 300,000 newly diagnosed cases in 2018. Non-melanoma cancer is the 5th most common cancer, and over a million people are affected by it.

Estimating the incidence of skin cancer presents a unique set of challenges due to a number of different factors. Because there are various kinds of skin cancer, it can be difficult to obtain accurate statistics on the disease. For example, non-

skin malignancies like melanoma are frequently overlooked by cancer registries. Melanoma is the worst form of skin cancer. This cancer registry is frequently inaccurate due to the fact that the vast majority of cases are curable by surgical procedures or excision.

Deep learning is an area of study within Machine learning. Convolutional Neural Networks enable the system to function by serving as its "brain.". In the past, we did not have access to a powerful personal computer, which made it difficult for us to provide the necessary data for the training of massive neural networks. On the other hand, Andrew claims that we now have computers that are fast enough to train a large number of neural networks. He also mentioned that supervised learning is where deep learning shines the brightest.

A type of technique for deep learning is known as a convolutional neural network (CNN). Convolutional neural networks frequently make use of a number of filters in order to retrieve picture attributes that are necessary for object categorization. CNN kernels extract these characteristics. Edge kernel identifies big pixel disparities. It analyzes a picture and gives importance to distinct shapes. CNN requires less preprocessing than others. CNN's advantage over its forebears is that it recognizes crucial features without human input. It is structured similarly to the neuronal connections seen in the human brain. We are now able to detect skin malignancies at an earlier stage with the assistance of a Convolutional Neural Network. This may be accomplished by providing the algorithms with a significant volume of data. When the learning algorithm is provided with an image, it will evaluate the image in accordance with its instructions and will look for a sample of skin cancer somewhere inside its own learning algorithm. If the results match those of the trained model, it will be possible to identify the specific form of skin cancer, making it simpler for patients to get curative treatment at an earlier stage.

The CNN U-net methodology was utilized for the purpose of data categorization. In order to obtain features, we made use of the Edge Histogram (EH), the Local Binary Pattern (LBP), the Gabor technique, and the Histogram of Oriented Gradients (HOG). The Support Vector Machine (SVM), the Naive Bayes classifier (NB), the K-Nearest Neighbor classifier (KNN), and the Random Forest classifier (RF) were all utilized in order to make an educated guess as to whether or not the provided picture depicted a lesion that was malignant or benign [29].

A CNN model consisting of more than 50 layers was utilized in order to accomplish the task of extracting differentiating features from the segments. Because their implementations of classification and segmentation took use of residual learning to minimize over-fitting, their classification and segmentation implementations received the best and second best result of segmentation and classification. This allowed them to avoid over-fitting. [28].

The conventional CNN convolutional block is changed in the following study, which is titled "Max-min convolutional neural networks for image categorization." In these research, the reputable data sources CIFAR-10 and MNIST are

utilized. According to the data presented, the convolutional neural network (CNN) beats its more traditional counterpart. Many deep networks might benefit from our Max-Min method with a few adjustments. [19].

Skin cancer photos have fine hairs and noise. Without processing, the picture will lose accuracy owing to reasons other than skin cancer. This work uses picture preprocessing methods. The study also used Karhunen-Loève (KL) transform histogram equalization. The study also emphasizes resizing all photos supplied to the algorithm to a fixed pixel width and variable pixel height. They denoised using wavelet denoise (by two-dimensional bior3.3 wavelet). This approach “blurs” images while keeping detail, therefore a Median filter was applied to reduce fine-hair noise [6].

## 1.1 Motivation

Skin infections cause skin cancer. Sometimes individuals don't identify the symptoms of skin cancer until it's too late. It's diagnosed via biopsy. It involves examining bodily tissue samples more carefully. X-rays show interior body components, but only a biopsy can reveal malignancy. It's uncomfortable and creates infection. It's time-consuming. Sometimes it doesn't show the correct result. Skin cancer causes 7% of new cancer cases globally.[3].Therefore, if you are able to diagnose skin cancer at a young age, you can treat this condition and protect yourself from further complications.

## 1.2 Research Problem

Skin cancer has been the most common form of illness seen around the world. Melanoma, often known as skin cancer, has been ranked as the 19th most common form of the disease in both men and women by the World Cancer Research . In 2018, it was reported that there were more than three-hundred thousand new cases. According to the most recent estimates, one out of every five people living in the United States will get skin cancer at some point throughout their lifetimes [4]. In the next decades, there has been an increase in the incidence of skin malignancies that are non-melanoma or melanoma. Over the course of the last several centuries, the number of people living in areas such as the United States, Canada, and Australia who have been diagnosed with skin cancer has increased by around one million people. According to research studies, it is estimated that more than 3 million people in the United States are diagnosed with non-melanoma skin cancer (NMSC) each year. This type of skin cancer comprises basal cell carcinoma (BCC) and squamous cell carcinoma (SCC).[8][13]. Between 1976-1984 and 2000-2010, the total incidence of basal cell carcinoma grew by 145 percent, while the overall incidence of squamous cell carcinoma climbed by 263 percent within the same time period.[25]. The incidence of both types of NMSC was significantly higher in females than to males.[25]Over a million people in the United States have been diagnosed with melanoma.[12].

It might seem that skin diseases have a significant detrimental effect on the overall health history of communities across the world. “According to the findings

of a study published in 2017, skin cancer is responsible for 1.79 percent of the global illness burden, which was calculated in disability-adjusted life years” [10]. There will be 196,060 new instances of melanoma identified in the United States in 2021, of which 101,280 will be considered mild cases and 106,110 will be considered aggressive cases [17][22]. It is expected that invasive melanoma will be the fifth most often diagnosed malignancy for both men and women in the year 2021, with a total of 62,260 cases for men and 43,850 cases for women [17][22]. Skin cancer accounts for around 7 percent of all newly diagnosed instances of cancer globally. [15], with a cost to the United States of almost 8 billion dollars in the year 2011 Medicare project. Clinical data shows race-related skin cancer outcome variations People with darker skin tones have a 20–30% greater chance of developing melanoma compared to those with lighter skin.; they also have a reduced or greater death risk for particular melanoma forms.

<b>Rank</b>	<b>Country</b>	<b>Rate scaled by ranks in 100,000</b>
1	Australia	33.6
2	New Zealand	33.3
3	Norway	29.6
4	Denmark	27.6
5	Netherlands	25.7
6	Sweden	24.7
7	Germany	21.6
8	Switzerland	21.3
9	Belgium	19.9
10	Slovenia	18.6
11	Luxembourg	16.5
12	Ireland	16.3
13	Finland	15.8
14	United Kingdom	15.0
15	Austria	13.6
15	France(metropolitan)	13.6
17	US	12.7
18	Czech republic	12.6
19	Canada	12.4
19	Italy	12.4

Table 1.1: Highest rates of skin cancer according to WCRF

“In recent times, Convolutional Neural Networks have widely been used for various classification and to classify skin cancer lesions” [20] .When it comes to the categorization of skin diseases, a great number of CNN models have significantly outpaced highly competent health care specialists.The efficiency of such models has been further enhanced by the application of a range of methodologies, such as transfer learning making use of vast datasets. This has led to an increase in the level of precision achieved.The VGG-16 and VGG-19 convolutional networks have 16 and 19, respectively, of their own convolutional layers.The pre-trained network was able to classify images such as a keyboard, mouse, pen, and critters into one thousand different levels of item categories. The networks have



developed exhaustive classification model for a vast array of images., and the resolution of the input data for those networks is 224-by-224. Additionally, the networks have amassed rich feature.

### 1.3 Research Objective

The risk of death from skin cancer is among the highest of any malignancy. It is expected to spread to other parts of the body if the first symptoms are ignored and the condition is not detected and treated. Additionally, the process occurs when the cells is exposed to direct sunlight, due mostly to the rapid growth of skin cells at this period. A robust automated system for the recognition of skin lesions is required for early detection in order to limit the amount of work, time, and risk to human life. Deep learning, computer vision, and image processing will all play important roles in the approach that will be taken to successfully cure skin cancer.

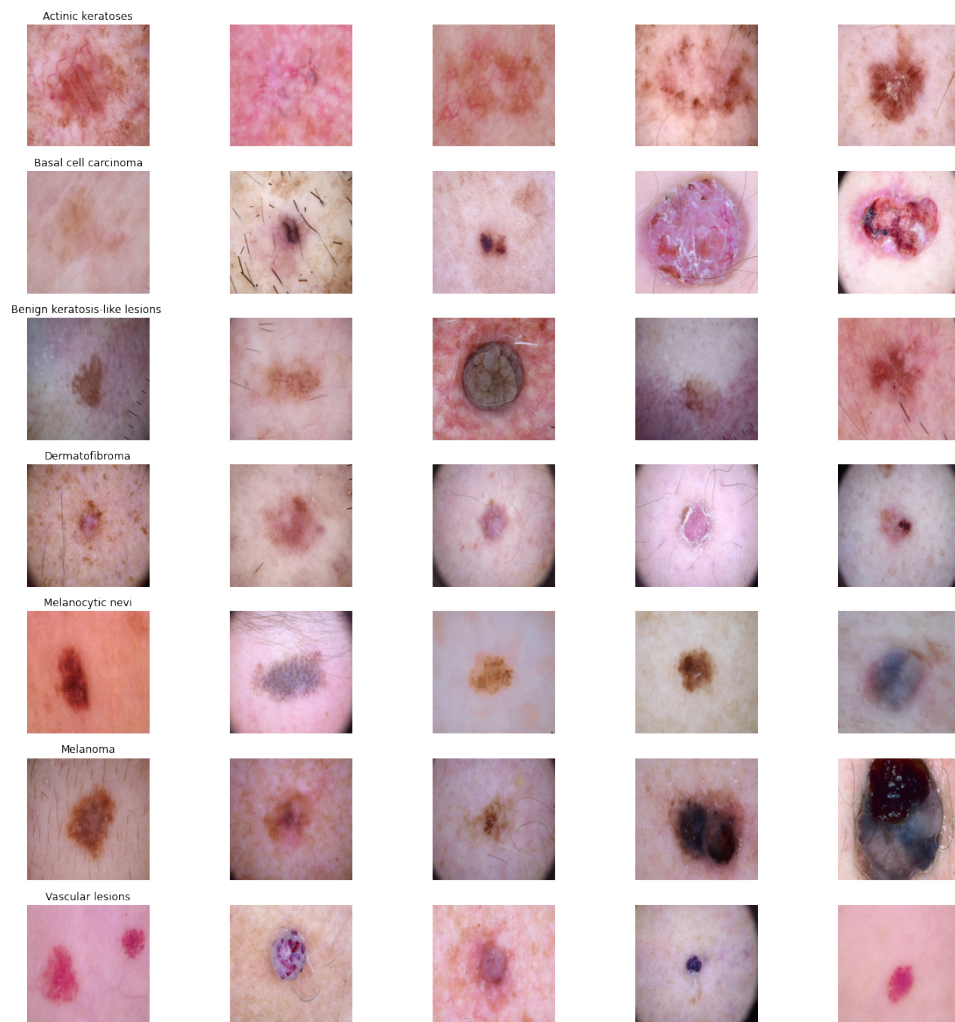


Figure1 : 7 types of skin cancer

In this article, a categorization of the seven distinct kinds of skin cancer will be explained. Additionally, the functionality and effectiveness of deep CNN will be evaluated and analyzed. Actinic keratosis, basal cell carcinoma, dermatofibroma,

melanoma, pigmented benign keratosis, and vascular lesions are the nine clinical forms of skin cancer that are included in the dataset. Through the use of the Convolution Neural Network, the primary objective is to develop a model that not only identifies cases of skin cancer but also categorizes them into a variety of subtypes. In the approach for diagnosis, the ideas of image processing, computer vision, and deep learning. The objective of this research are:

1. Observing deep convolutional neural networks (CNN).
2. Create a reliable automated method for recognizing skin lesions as soon as possible.
3. Create a model using the CNN that not only diagnoses skin cancer but also classifies it into the numerous subtypes that it can take.
4. To analyze model.
5. Compare the base models with the concatenated models.
6. To offer recommendations on improving the model.

# Chapter 2

## Literature Review

The acronym "CNN" stands for "Convolutional Neural Network." The network solves problems using a convolutional system of linear equations, which is where the term "convolutional neural network" gets its meaning. In at least one of its layers, this type of neural network substitutes matrix convolution for the more fundamental operation of matrix multiplication. Deep learning makes use of a specific sort of artificial neural network known as a convolutional neural network, sometimes abbreviated as CNN or ConvNet, to evaluate visual data. CNN is a form of deep learning approach for processing data with a grid pattern that is produced automatically and adaptively. This pattern is inspired by the architecture of the animal visual brain and was designed by CNN. Input layer, concealed layer, and output layer are all components of this layered structure. Image processing, classification, and segmentation are among its most common applications, along with other types of auto-correlated data. CNN has a fundamental advantage over its competitors due to the fact that it can identify significant traits without the intervention of a human being. If it is shown a huge number of pictures of cats and dogs, it can figure out on its own the specific qualities that are unique to each class. For example, Convolutional Neural Networks start with a picture, then break it up into numerous layers, search for matches with the data that they are supplied, and seek to provide the most results that are maximally matched. In addition to this, CNN has a low computational overhead. But there is no denying that it also comes with a few drawbacks. For instance, it requires a significant quantity of data for training and does not save the location or orientation of the objects being analyzed.

There is a wide variety of CNN models to choose from. CNNs that are used frequently include LeNet, AlexNet, ResNet, GoogleNet, InceptionNet, MobileNetV1, ZfNet, Depth-based CNNs, Highway Networks, Wide ResNet, VGG, PolyNet, Inception v2, Inception V3 V4, and Inception-ResNet; DenseNet; Pyramidal Net; Xception; Channel Boosted CNN using TL; Residual Attention NN; Attention Based CNNs; Feautre-Map based

A tensor of shape is what feeds into a CNN as its input. A tensor is a mathematical construct that is similar to but significantly more general than a vector. It has been described by a collection of components that are functions of the coordinates of a space. After going through a convolutional layer, the image is

transformed into an abstract form known as a feature map, which has shape. It would require an extremely high number of neurons, even in the most fundamental of models, because the input size of photos is so big, and because each pixel is such a significant attribute. Following this, each neuron computes an output value by applying a predetermined function to the input values that it has received from the receptive field of the layer below it in the hierarchy.

In order to train and evaluate deep learning CNN models, each input picture will be processed by a series of convolution layers that include filters (Kernels), Pooling, fully connected layers (FC), and the Softmax function. The goal of this process is to identify an image with probabilities values that range from 0 to 1, and it will be done in order. In practice, CNN is only useful for viewing photos. It is possible to add it to any 2D or 3D array. The convolutional layers are the layers that are added to the neural network before the layout is done. Convolution layers are used to increase the computer's ability to recognize qualities that would otherwise be lost if an image were only transformed into pixel values. These characteristics would be lost if the picture were translated into pixel

**VGG-19:** Visual Geometry Group is an example of a multilayered deep Convolutional Neural Network (CNN) architecture. Since VGG-19 contains 19 convolutional layers, the term "deep" refers to the total number of layers in the model. It is a highly developed CNN with layers that have already been trained. The VGG19 model, often referred to as VGGNet-19, is comparable to the VGG16 model; however, it consists of 19 layers instead of 16. When compared to VGG16, VGG19 contains three more convolutional layers. In its most basic form, it is an advanced form of object recognition. One of the most difficult picture recognition systems ever devised uses this method. There are about 138 million different parameters, and its accuracy is said to be 92.7 percent [27]. Although VGG19 is somewhat larger than VGG-16, VGG-16 is essentially identical in capabilities to VGG19.

**ResNet50:** The term "ResNet" stands for "Residual Network," which serves as the central support structure for a variety of computer vision activities. It possesses more than 150 layers, which make it possible to train the deep neural network. Back in 2015, Kaiming Within the scope of his work, he initially presented ResNet. As deep optimized learning training takes twice as long and is limited to a specific number of layers, this design was created to overcome some of the technique's challenges. It is possible to utilize ResNet in order to bypass connections or take shortcuts, which is the reason for its complicated design. In addition to the performance of other architectural models, the performance of the ResNet model does not improve as the complexity of the design increases. Additionally, the difficulty of computing calculations has been lowered, and the ability of training neural networks has been improved. Skipping connections between two- to three-layer architectures using ReLU as well as batchNormalization enables the system of the ResNet model. In order to finish the remaining ResNet block, it is necessary for both the input and output data dimensions to be the

same. In addition, each ResNet block is comprised of either two or three layers (for ResNet-18 and ResNet-34 networks, respectively) (for ResNet-50 and ResNet-101 networks). The initial two levels of the ResNet design closely resemble GoogleNet. “These layers make use of convolution 7 x 7 and max-pooling with size 3 x 3 and stride number 227” [24].

**Keras:** Keras is a software package that is available under an open-source license that offers a python interface for an artificial neural network. It is compatible with a number of different back-ends, including as TensorFlow, Microsoft Cognitive Toolkit, Theano, and PlaidML. An engineer at Google by the name of Francois Chollet was the one who developed and continues to maintain it. Keras is composed of several distinct sorts of layers. Layers with names like “Dense layer,” “Flattened layer,” “Dropout layer,” “Reshape layer,” “Permute layer,” “Lambda layer,” and “Pooling layer” are all examples. It is essentially a robust and user-friendly Python library that is open source and free, and can be used for the development and evaluation of deep learning models. For developers, Keras is a more user-friendly option than TensorFlow. Learning keras is significantly more straightforward for first-timers. It is an application programming interface (API) designed for human beings, not for machines. It is built on a straightforward structure, which contributes to the creation of a straightforward method for building deep learning models.

**TensorFlow:** It is a free and open-source library for artificial neural networks. It’s a symbolic math library based on data flow and differentiable programming. It comes with a set of processes for creating and training models in Python or JavaScript, as well as deploying them in the cloud, on-premise, in the browser, or on mobile devices, independent of the language. The tf. data API lets you to combine modules to produce massive input streams. The most important thing to remember about TensorFlow is that its core is mostly not written in Python: For best results, it’s written in a mix of C++ and CUDA. It’s a machine learning platform that’s open source from start to finish. For computer vision problems, the open source TensorFlow framework enables for the creation of highly flexible CNN architecture. TensorFlow is used for a variety of tasks, including speech recognition, sentiment analysis, language identification, text summarization, picture recognition, video detection, time series, and more. TensorFlow is difficult to learn and much more difficult to use, according to users and industry specialists. TensorFlow is well-known for its lack of flexibility, yet research is all about flexibility, which is why mastering it is challenging. It may be used for a variety of purposes, not simply deep learning. The caller driver of the tensor flow graph built with the C++ API can use a client session object. TensorFlow, in a nutshell, makes machine learning simple. Because of pre-trained models, data, and high-level APIs, anybody can now develop ML models. The following words are commonly used by researchers: The majority of academics and students utilize TensorFlow in their analysis and model construction.

**Concatenate:** The term "concatenation" refers to the process of joining together two separate layers of strings. It receives as an input a list of tensors that are all the same shape with the exception of the concatenation axis, and it outputs a single tensor that is the concatenation of all of the tensors that were given as input.

**Inception V3:** It has been proven that the picture recognition model known as Inception v3 can reach an accuracy that is greater than 78.1 percent when applied to the ImageNet dataset. The model is the product of several concepts that were developed over the course of time by a number of different scholars[9]. There are both symmetric and asymmetric construction components included in the model. Some examples of these are convolutions, average pooling, max pooling, concatenations, dropouts, and completely connected layers. The batch normalization process is employed extensively throughout the model and is performed in order to activate inputs. The calculation of loss is done with softmax.

**API:** Application Programming Interface is the full version of the abbreviation API. It is a collection of definitions and protocols for constructing application software and integrating it with other programs. An application is a generic term for any computer software that was designed to do a certain task. One way to conceptualize an interface is as a service agreement made between two different applications. This agreement details the manner in which the two will communicate by exchanging questions and responses. APIs are essential for connecting apps so that they may carry out a predetermined purpose, which may involve the exchange of data and the execution of predetermined operations. They help developers to establish new programmatic interactions by acting as a bridge between the many programs that individuals and organizations use on a regular basis and the programs that are developed by the developers themselves. Keras is an application programming interface (API) for deep learning that is written in Python and runs on top of TensorFlow, a platform for machine learning. It was constructed with the purpose of making quick experimentation easier to do. When doing data collection, it is essential to be able to proceed from the concept to the conclusion as quickly as is humanly feasible. It is not employed for machines but rather for people. The ideal criteria are utilized by Keras in order to reduce cognitive strain.

The functional API is able to handle models with non-linear topologies, shared layers, and even numerous inputs and outputs from a single model. According to the core principle, a deep learning model is frequently a directed acyclic graph (DAG) of layers. In conclusion, you are able to create layer graphs by making use of the functional API. On the other hand, the Sequential API gives you the ability to build models by stacking them one on top of the other, step by step. It is restricted in the sense that it does not enable the creation of models with several layers or inputs and outputs. This is one of its limitations. The primary distinction between these two application programming interfaces (APIs) is that the functional API provides users with greater control and flexibility over the layers than the sequential API does.

- **Functional API:** Keras' functional API provides model definition flexibility. It creates models with multiple inputs or outputs and shared layers. It creates informal polycyclic network graphs. Models are formed by constructing layers and connecting them in pairs, then defining a Model that specifies the input and output layers. Unlike the Sequential approach, one must design and construct an independent Input layer. The input layer receives a shape parameter that sets the data's dimensions. When training a multilayer Perceptron with one-dimensional data, the shape must include the mini-batch size. The shape tuple always has a dangling last dimension for one-dimensional input.

The model's layers are connected in pairs. Define each additional layer's input source. After a layer is built, its input layer is denoted using bracket notation. Here's an example. Make the input layer as stated above, then a Dense hidden layer that only receives input from the input layer.

After linking all model layers, declare the model. The model may be summarized, fitted, assessed, and used to make predictions, like the Sequential API. Keras' Model class may construct a model from your layers. Input and output layers must be defined.

- **Sequential API:** It is really straightforward and simple to operate. Stacking the models gives you the ability to develop models in a layer-by-layer fashion. However, the primary issue with using this API is that it is difficult to design models that have several inputs, outputs, or common layers. There is no flexibility in the Merge Layers, Concatenate Layers, or Add Layers operations in a network.

## 2.1 Related Work

This part mainly focuses on the reviews of previous relevant works. Here we use CNN, VGG-19, and others to detect skin cancer. We have analyzed quite a few models to get an accurate result.

"Softmax," is used as the final layer as it is a form of logistic regression that normalizes an input value into a vector of value [23][26]. "Aging in 'AlexNet' is used as it allows for multi-training GPU by putting half of the model's neurons" [23][26].

Using CNN is that it needs extensive training data and does not encode the object's position. It also cannot encode the orientation of the object.

A recent work [14] uses all RF, SGD, SVM, VGG-19, VGG-16, and Inception-V3. It shows that VGG-16 works better than RF.

According to [23], "In this paper, a pre-trained deep learning network and transfer learning are utilized (AlexNet) and replacing the last layer by "softmax" to classify three different lesions (Melanoma, atypical nevus, and common nevus). Ph2 dataset is used to test and train the proposed model. Two experiments were done, with and without augmentation of pictures. Four performance measures have been computed for the proposed model to compare with existing methods, where the obtained results prove that the proposed model outperformed the existing methods. The achieved rates are 98.61%, 98.33%, 98.93%, and 97.73% for

accuracy, sensitivity, specificity, and precision”.

From [26], this paper mainly focuses on how they made the prototype and how it works over the servers and the remote device. We only want to study the data training part from this and the tuning of the algorithm. Initially, three extremely deep convolutional neural networks are pre-trained using the image database known as ImageNet. Then a fine-tuning is carried out on all layers. The last layer is the softmax layer, which allows classifying two diagnosis classes. In the entire experiment, the learning rate is to be set at 0.001, and the batch size is to be 150. In conclusion, it can be seen from the statistical data that the AlexNet model has the best overall effect.

From [18], “ In this paper, classification of skin lesions is demonstrated using a single CNN (GoogleNet Inception v3 CNN ), trained end-to-end from images directly, using only pixels and disease labels as inputs and compared against dermatologists. CNN is trained using a dataset of 129,450 clinical images. In all tests, the CNN outperforms all tested specialists, proving that artificial intelligence can classify skin cancer at a level of expertise comparable to dermatologists. The CNN obtains overall accuracy (the average of individual inference class accuracies) of 72.10.9% (mean s.d.) in this job. In comparison, two dermatologists score 65.56 percent and 66.0 percent accuracy on a subset of the validation set”. According to [7], this paper aims to detect cassava diseases with a CNN dataset with 99.53% of accuracy. AlexNet, AlexNetOWTBn, GoogleNet, Over-feat, and VGG datasets with 87848 images were used to detect the diseases. Three convolution layers were also used. Though it has some challenges regarding small dataset, color resolution, and class label skew, its primary goal was to maximize performance by minimizing the computational time.

According to [14], this paper focuses on plant disease detection with various types of Machine learning and Deep learning methods. However, DL methods perform better than ML methods in detecting plant diseases. The accuracy is RF-76.8% , SGD-86.5% , SVM- 87% , VGG-19-87.4% , Inception-v3-89% , VGG-16-89.5%. DL and ML work similarly, but DL results tend to be more accurate

According to [21], this paper focuses on artificial skin cancer-detecting with the help of image processing, machine learning, and deep learning methods. The accuracy is about 89.5%, and the training accuracy is 93.7%. Neural Networks were used to detect benign and malignant, and CNN was used in signal and image processing. CNN can detect cancerous cells more quickly and effectively.

From [5], in this paper, they have given a survey that reflects an intersection of Computer Vision and medicine, which focuses on research in medical imaging, medical video, and accurate clinical deployment. Here, they used Data Learning techniques and computer vision and tried to explain how to detect the disease. They explained that people should use CNN and MIL and massive 3D pictures (res. 100000\*100000) to detect medical solutions. It will perform better than CNN, which usually takes 2D (200\*200) pictures and output.

From [1], the paper shows that the author used Lesion segmentation for detecting Melanoma in dermoscopy images. Here they described the drawbacks of lesion segmentation and how to overcome those drawbacks. In the preprocessing steps of LS, they eliminated the carryable lighting effects they have in a conventional picture and included different color channels, enhanced the contrast, normalized the picture, and eliminated vintage effects from the picture to detect accurately.



Moreover, they have shown feature segmentation that uses lesion segmentation for the picture, making the picture a bit brighter and sharper. It uses the same techniques as LS.

## 2.2 Seven Types of Skin Cancer

Sun-exposed skin means that the vast majority of incidences of skin cancer, which can be defined as an abnormal cells of skin cells. However, this type of cancer, which is rather frequent, can develop in parts of the skin that are only sometimes exposed to the sun. Because of these flaws, skin cells grow in an uncontrolled manner, which ultimately results in human cancers. The most common types of skin cancer are basal cell and squamous cell. Melanoma and Non-melanoma. In the course of our inquiry, we will be looking into seven different kinds of skin growths and lesions.

- Actinic keratosis and intraepithelial carcinoma (akiec)
- Basal cell carcinoma (bcc)
- Benign keratosis-like lesions (bkl)
- Dermatofibroma (df)
- Melanoma (mel)
- Melanocytic nevi (nv)
- Vascular lesions (vasc)

Below, we'll go deeper into the many sorts of skin lesions and growths.

### 2.2.1 Actinic Keratosis and Intraepithelial Carcinoma

Actinic keratoses (AKs), sometimes called senile keratosis or sun keratosis, are benign intraepithelial growths that are one of the most frequent fungal diseases evaluated by dermatologists. Actinic keratoses are caused by exposure to the sun. People who have AKs are more likely to develop irregular, red, scaly papules or plaques on sun-exposed parts of their bodies, which is a symptom that is often linked with prolonged sun exposure. Because AKs have the potential to develop into widespread squamous cell carcinoma if they are not treated, the need of making an early detection and developing a treatment plan cannot be overstated.

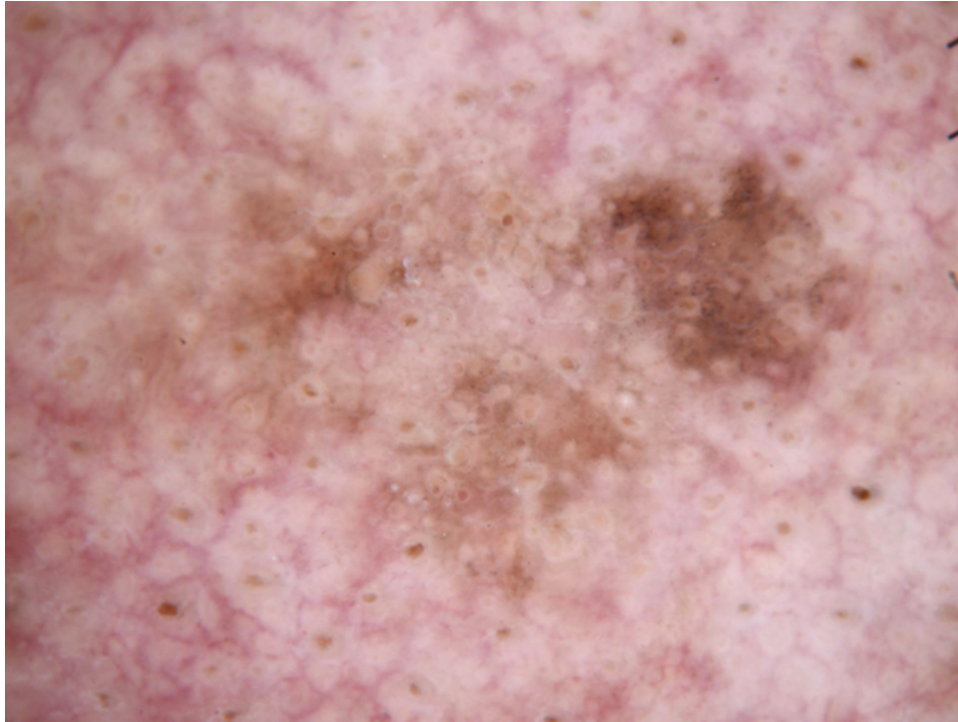


*Figure 2: Actinic Keratosis*

There are five different types of actinic keratoses: hypertrophic, atrophic, bowenoid, cantholytic, and pigmented actinic keratoses. Hypertrophic actinic keratoses are the most common. The hypertrophic and atrophic forms are the ones that are seen most frequently. In its most basic form, actinobacillus keratosis (AK) is a kind of keratinocyte skin cancer that results from prolonged exposure to the sun. Actinic keratoses can be split into two distinct categories.

- Pigmented Actinic Keratosis: Actinic keratosis can also take the form of pigmented actinic keratosis, which is a less frequent variant. It is possible that, rather than growing into an erythematous plaque, it would seem more like a pigmented or keratinocytes lesion (also known as lentigo maligna or solar lentigo) (lichen planus-like keratosis). The signs of this kind of AK include irregular follicle openings and the formation of gray specks arranged in symmetrical arrangements between follicular structures. This form of AK is more frequent in those with darker skin. They produce a significant pseudo-network that connects all of the affected follicular structures in the area.
- Non Pigmented Actinic Keratosis: The term "strawberry pattern" refers to the appearance that non pigmented actinic keratosis has on the face. The substantial UV damage that many patients have endured often results in the lesion's boundary being well-defined; yet, it is possible for it to blend in with the skin that is around it. One possibility is to use a pink backdrop that is unstructured. Essentially, it contains four characteristics that allow for a highly precise and specific diagnosis:
  - Vessels that are fine and wavy
  - Targetoid hair follicles

- Erythema
- Pink-to-red pseudo-network

## 2.2.2 Basal Cell Carcinoma

The most common place for a person to get basal cell carcinoma(BCC), is on an area of their body that is frequently exposed to the sun, such as their face. On dark brown or black skin, a brown or glossy black lump with a rolled border is the classic expression of basal cell carcinoma. This particular kind of melanoma is known as basal cell carcinoma. This factor is responsible for around 80% of all cases of skin cancer. Although it is not commonly fatal, it may be rather aggressive in certain areas.



*Figure 3: Basal Cell Carcinoma*

There are 5 symptoms of Basal Cell Carcinoma:

- Sores that seem to be open
- a pale and irritated skin
- Shiny nodules
- Excessive Growths
- Scars that are visible

BCC accounts for nearly one-third of all skin cancer diagnoses in the U.S. In certain cases, cancer can migrate to adjacent tissue and bone.

### 2.2.3 Benign Keratosis-like Lesions

Seborrheic keratosis (Benign keratosis-like lesions) are noncancerous skin growths. People have a tendency to have more children as they get older. The color of a seborrheic keratosis can typically be described as brown, black, or light tan. The lesions are high, and they have a glossy or smooth appearance. Although it is most often seen on the back or chest area, it can manifest itself anywhere on the body.

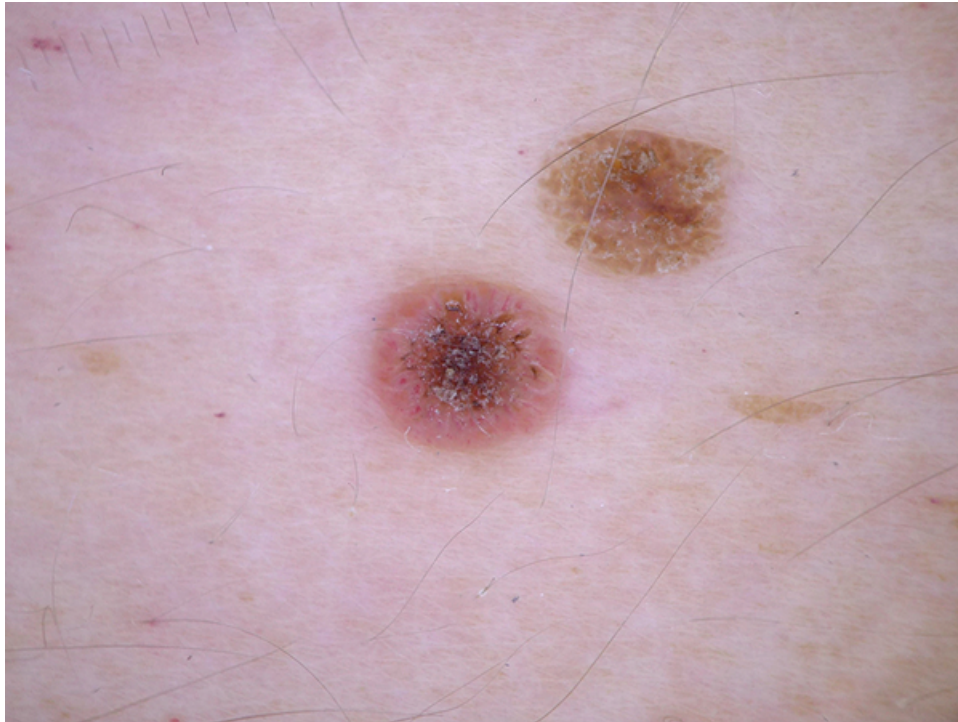


*Figure 4 : Benign keratosis-like lesions*

In the general population, seborrheic keratoses are relatively prevalent, affecting an estimated 90 percent of people over the age of 30. However, seborrheic keratoses are extremely rare in people under the age of 20, therefore it is important to be aware of this fact. The lesions eventually spread to every region of the body as time went on. Because these keratoses can appear everywhere on the skin, including non-seborrheic regions, the word may lead to confusion.

## 2.2.4 Dermatofibroma

Dermatofibroma, also known as superficial benign fibrous histiocytoma, is a common benign skin tumor that affects women to a far greater extent than males. Dermatofibroma most frequently affects the extremities, and more specifically the lower legs. Although the condition is asymptomatic, patients may experience itching and discomfort. In contrast, the color of a person's skin can range anywhere from pink to brown depending on their level of fairness or darkness. These growths have a significant feel to them, much like a little stone or lump that has developed skin over them. The dimpled skin that surrounds dermatofibromas is one of the characteristics that distinguishes them from other growths.

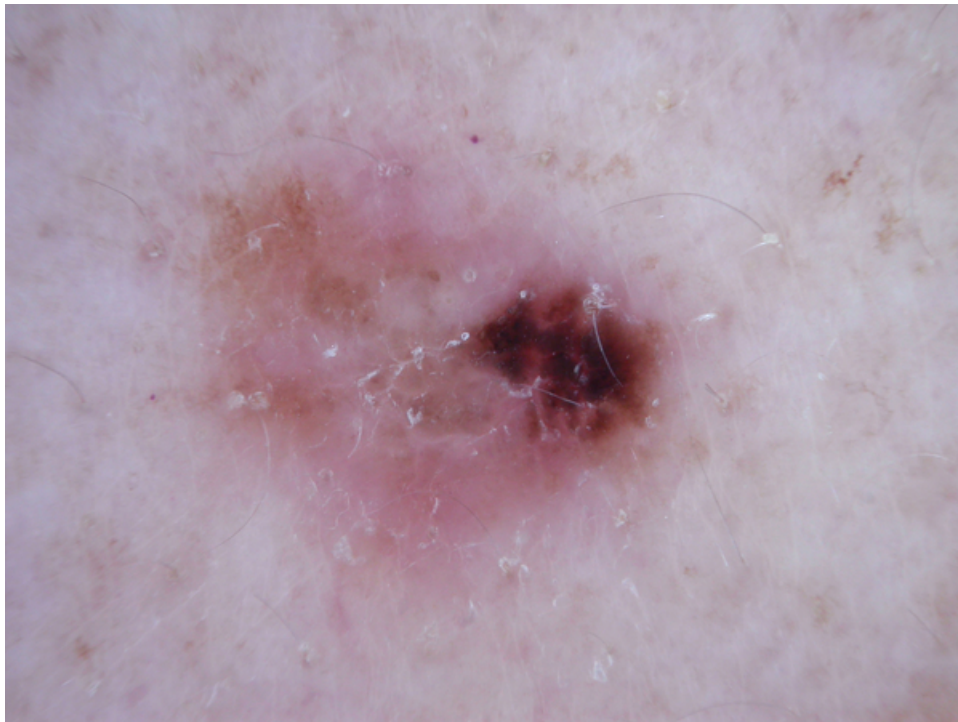


*Figure 5: Dermatofibroma*

## 2.2.5 Melanoma

Melanoma is a form of skin cancer that originates in the cells that give your skin its color. Melanomas tend to spread quickly (melanocytes). It is possible to observe the progression of melanoma cells from the surface of the skin into the deeper layers. Melanocytes are cells that are found in our skin and eyes. Melanin is the pigment that is responsible for our appearance, and melanocytes produce and store it. Melanoma is most commonly caused by overexposure to ultraviolet (UV) radiation, which can occur both naturally and artificially in tanning beds and sunlight. The risk of developing melanoma is proportional to the amount of time spent in UV light. Early sun exposure is one of the most important risk factors for developing melanoma, and this is especially true for people who suffered from severe sunburns as children. UV radiation may induce damage to DNA, which can lead to uncontrolled cell development in melanocytes and ultimately melanoma. This is the case for all forms of skin cancer, including melanoma.

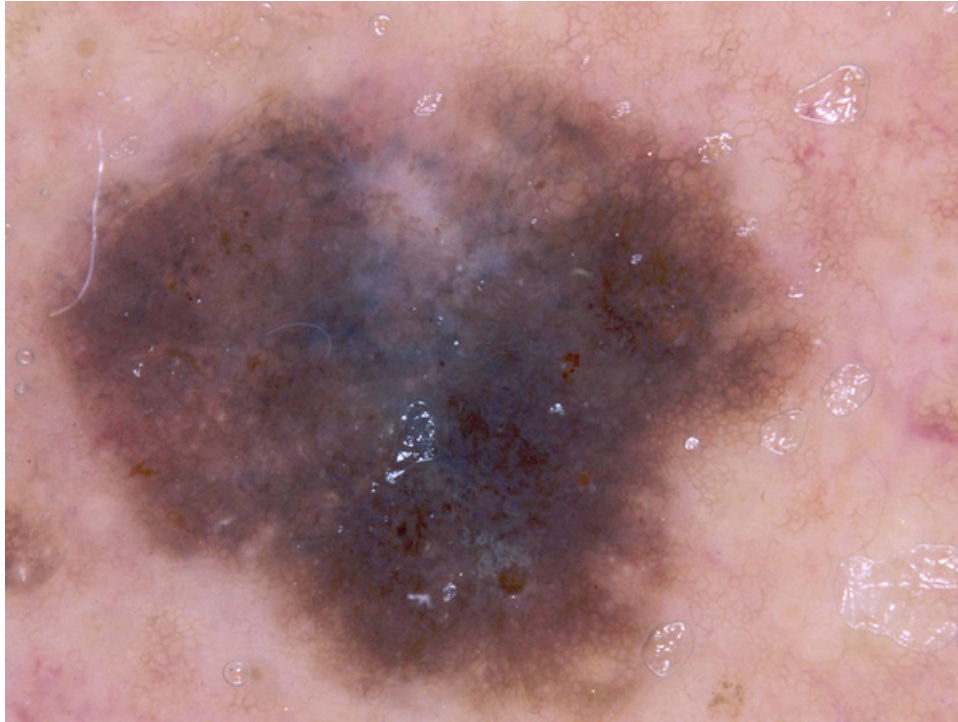


*Figure 6 : Melanoma*

Beyond-spot pigmentation, redness, or inflammation. Itching, soreness, or pain may occur. Changes in a mole's texture or scales, bleeding. Symptoms include blurry vision, partial blindness, and black iris patches. Melanoma has 4 primary subtypes.

- Nodular
- Lentigo Malinga
- Acral lentiginous
- Superficial Spreading

A biopsy of the suspicious area of skin, also known as a lesion, is the only way for the doctor to determine whether or not it is cancer. A tissue sample is taken and examined under a microscope in a clinical setting; this procedure is referred to as a biopsy.

### **2.2.6 Melanocytic Nevi**

Melanocytic nevi are a type of hamartoma or benign neoplasm that are composed of melanocytes. Melanocytes are pigment-producing cells that regularly populate the epidermis. Melanocytic nevi can be found anywhere on the body. Melanocytic nevus is a benign skin lesion that is created by the proliferation of pigmented cells known as melanocytes. Melanocytic nevi can range in size from a few millimeters to several centimeters. Moles can be found on almost any part of the body. The aggregation of melanocytes is what leads to the development of black moles, which can appear on both men and women at any age. They might be present at birth, or they could be something that develops through time.

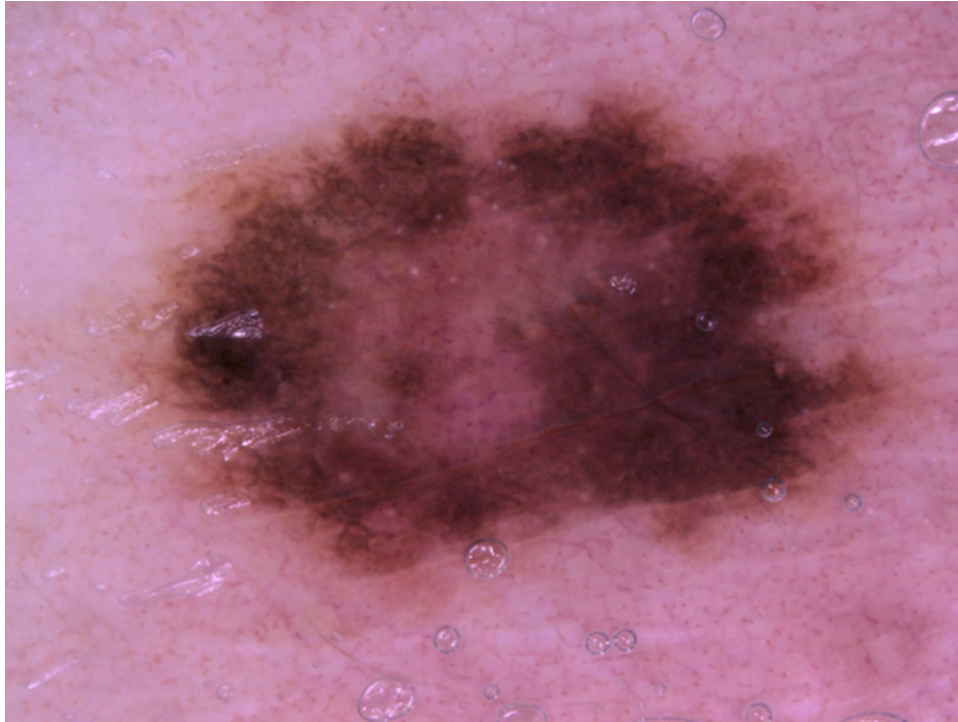


*Figure 7 : Melanocytic nevi*

Hereditary factors and sun exposure may produce melanocytic nevi. Melanocytic nevi may enlarge and depigment, changing color and form. People with more nevi are more prone to acquire melanoma. One in 75 persons and one in 20,000 newborns have small melanocytic nevi. Melanocytic nevi are not the same as melanoma, a deadly skin cancer. Nevi have a symmetrical form, unlike melanoma.

### **2.2.7 Vascular Lesions**

Birthmarks are a common name for a group of skin and tissue anomalies that can appear on people of any age, regardless of the color of their skin or gender, and can affect any skin tone. Vascular lesions, more often known as birthmarks, are extremely common types of skin and underlying tissue abnormalities.



*Figure 8 : Vascular lesions*

The three most common forms of vascular lesions are known as hemangiomas, vascular malformations, and pyogenic granulomas.

- Hemangiomas: At birth, they show as whitish or reddish patches on the skin, which are followed by fast increase in size and thickness throughout the course of one's lifetime. These growths are benign tumors of the cells that coat blood vessels. This can lead to ulceration, which is defined as a break in the top layer of the skin, as well as bleeding (and, in the worst-case scenario, infection). They have rapid expansion throughout the first six to twelve months of their lives, after which their size level off, gradually decrease, and they finally pass away. Hemangiomas of the eyelid have the potential to cause irreversible blindness in certain newborns.
- Pyogenic Granulomas: When there is damage to the skin tissue in one specific area, benign vascular lesions of the skin can develop. They develop very quickly, generating red spikes that resemble tumors and eventually lead to ulcers that are highly bleedable. This kind of vascular lesion is found in a disproportionately high number of children and women who are pregnant.
- Vascular Malformations: Vascular malformations are a type of congenital vascular abnormality that can affect either just the veins, just the lymph vessels, both the veins and the lymph vessels, both the arteries and the veins, or both of these. Only the veins themselves are affected by venous malformation (VM) Only lymph vessels are impacted when lymphatic dysfunction occurs (LM).



# Chapter 3

## Data Description

In order to train a neural network-based approach, it is important to have access to a huge number of pictures that have been sorted and categorized. Therefore, in order to deliver reliable diagnoses of high-quality dermatoscopic photos, the sources providing those diagnoses need to follow to size and accuracy constraints.

The findings of recent research (Tschandl et al., 2018) combine data gathered from a diverse range of demographic groups over the course of twenty years using a variety of different approaches to data collecting. The “Department of Dermatology at the Medical University of Vienna” in Vienna, Austria, and Cliff Rosendahl’s skin cancer center in Queensland, Australia, are two major sources. Both of these institutions are located in Austria. This dataset includes a total of 10,015 dermatoscopic simulacra, the ISIC repository and the Harvard Dataverse both make all of these datasets accessible to the general public so that they may be used in academic machine learning research. The dataset acts as a testing ground for machine-learning methods. The data collection contains representations for the seven basic diagnostic criteria used to classify pigmented growths or lesions.[16].

Measurement Type(s)	Skin lesions
Design Type(s)	Data integration objective; Dataset creation objective; Image format conversion objective
Sample Characteristic(s)	Humans ; skin on the body
Factor type(s)	Type of Diagnostic procedure; Age ; Biological sex; Body part
Technology Type(s)	Digital curation

### 3.1 Dataset Background

Examination of pigmented skin lesions with the naked eye is not sufficient for making an accurate diagnosis of benign or malignant pigmented skin lesions; dermatoscopy, a frequently practiced diagnostic method, is superior in this regard. Dermatoscopic pictures may be utilized in the training of artificial neural networks, which enables the development of diagnostic systems that are capable of automatically identifying pigmented skin growths or lesions.

“In 1994, Binder had had achieved his goal of effectively training an artificial neural network to differentiate melanomas, the most lethal form of skin cancer, from melanocytic nevi by making use of dermatoscopic photographs” [11]. The findings were positive; however, the sample size was small, and there were no

dermatoscopic photographs of anything other than melanoma and nevi. This was a problem that existed in the majority of the earlier research as well. In recent years, improvements in graphics cards and techniques for machine learning have enabled the creation of stronger and more complicated neural networks, which has allowed for the enhanced and more efficient automatic detection of pigmented skin growths and lesions.[2].

The ISIC archive presently comprised of around 23,665 photos as of April 2020. Because of its more flexible authorization (CC-0), its more organized access, and its bigger size, it has become the key resource for research on dermatoscopic image analysis. On the other hand, it is more likely to develop melanocytic lesions .

Abbreviation	Class	No. of Images
akiec	Bowen disease	334
bcc	Basal Cell Carcinoma	583
bkl	Benign Keratosis-like lesions	1674
df	Dermatofibroma	122
nv	Melanocytic Nevi	18,618
mel	Melanoma	2177
vasc	Vascular Lesions	157
		Total=23665

Table 3.1: Overview of ISIC archive and Class Distribution upto April 2020

## 3.2 Dataset Classification

Over the course of twenty years, the “dermatology department of Medical University of Vienna” in Austria and the clinic of skin cancer run by Cliff Rosendahl in Queensland, Australia, have collected photographs to the HAM10000 database. On the Australian website, PowerPoint records and Spreadsheets databases were used to store the meta-data and photographs that were saved for preservation, respectively. The Austrian website started collecting visual evidence long before the mass availability of digital cameras, and it has consistently preserved both photos and information in a wide range of file types ever since. It was necessary to organize and classify the data into a single format in order to guarantee that it would be consistent and easy to access it. Among the several methods utilized were[16]:

- PowerPoint files are being exploited for graphics and metadata:The monthly clinical reports and photos from a skin cancer practice in Australia were compiled into separate PowerPoint files, one for each month of the calendar year in which a patient was diagnosed with skin cancer. These PowerPoint files may be downloaded here. Python was used to build a computerized system that included a single picture, a comment, and other unique identifying information on each monthly slide. This system was constructed automatically. Because there was such a massive amount of data, we had to resort to an automated method in order to extract and organize those photos.

- The digitization of the Dispositive: Digitization converts information to a digital format. Dispositive is a translucent photograph. Long before the invention of digital cameras, Dermatology images in Austria were conclusive. With something like a Nikon Coolscan 5000 ED and Digital ICE, we recognized the dispositive and saved the files as JPEG Images of the best quality (300DPI; 1510 cm). Manually cut scanned photographs to 800x600px @ 72DPI with the lesion centered, then did histogram tweaks to increase contrast and color accuracy.
- Information Extraction from a Digital Dermatoscopy Method: Years after digital cameras were first released, the Department of Dermatology decided to move to the MoleMax HD system, which is a digital dermatoscopy system. The study only included non-melanocytic lesions that had a consensus benign diagnosis, nevi that had more than one and a half years of digitized dermatoscopic follow-up, and excised lesions that included a histopathologic result. A manual process was utilized in order to link histopathologic results to individual lesions.
- Image filtering for dermoscopy: All radiographs, including dermatoscopic and clinical close-ups, were taken by medical professionals. As dermatoscopic radiographs lack a sufficient source annotation, they must be manually separated from the remaining radiographs. The 1,501 radiographs contained in the Australian data set were categorized manually into three categories: overviews, close-ups, and dermatoscopy. After manually labeling the photographs, they were utilized to train an ANN to automatically label the image data. The stated accuracy of 98.68% accelerated the categorization of future radiographs for the HAM dataset, which was followed by a second manual review to reduce misclassifications.
- Pathology unification: Misspellings, distinct dermatopathologic words, multiple diagnoses per lesion, and unclear diagnoses leads to extra histopathologic diagnoses across sites. Injuries and unclear diagnoses were removed, apart from melanomas with lesions.

With the exception of melanomas and nevi, all of the ambiguous diagnoses have been removed. The remaining diagnoses were partitioned into seven (7) different generic categories so that there would be no room for doubt in the generalization process. As will be discussed in greater detail below, these groups contained greater than 95 percent of all growths and pigmented lesions that were reported at both data retrieval locations. [16].

### 3.3 Dataset Sources and Comparisons

Every single data record that is contained in the HAM10000 dataset may be found in the Harvard Data Set. Photos and metadata were donated to this project by the ViDIR Group at the University of Queensland . The project is licensed under the “Creative Commons Attribution-Noncommercial 4.0 International Public License”. The following table lists dermatoscopic image datasets that are available to the general public. These datasets include the PH2 and the Interactive Atlas of Dermoscopy. Additionally, the table includes information on the HAM10000 dataset that was employed in our research..

Dataset	License	Total Image	Pathologic Verification (%)	akiec	bcc	bkl	df	mel	nv	vasc
<b>HAM10000</b>	CC BY-NC 4.0	<b>10015</b>	<b>53.3%</b>	327	514	1099	115	1113	6705	142
PH2	Research & Exhibition	200	20.5%	-	-	-	-	40	160	-
Rosendahl	CC BY-NC 4.0	2259	100%	295	296	490	30	342	803	3
ViDIR Legacy	CC BY-NC 4.0	439	100%	0	5	10	4	67	350	3
Atlas	No License	1024	Unknown	5	42	70	20	275	582	30
ViDIR Current	CC BY-NC 4.0	3363	77.1%	32	211	475	51	680	1832	82
ViDIR MoleMax	CC BY-NC 4.0	3954	1.2%	0	2	124	30	24	3720	54
ISIC 2017	CC-0	13786	26.3%	2	33	575	7	1019	11861	15

Table 3.2: Comparison of HAM10000 with other datasets containing dermatoscopic images that are openly available.

#### 3.3.1 Rosendahl Image Set

The University of Queensland’s School of Medicine’s CR (Cliff Rosendahl) skin cancer department donated data for the Rosendahl component of the HAM10000 dataset. A non-polarized DermLite Fluid or DL3 with soaking solution was used by author CR (70 percent ethanol hand-wash gel or ultrasonic gel) [16]. We gathered 36802 histopathologic photos from a total of 34.2GB worth of digital slides from Rosendahl (122 PowerPoint™-files). We were able to arrive at the final dataset by removing non-pigmented lesions, overviews, close-ups that did not include dermatoscopy, and occurrences that did not have a diagnosis or had an incorrect diagnosis and did not fall into one of the predefined broad groups, as shown in the figure [Table 3.2].

#### 3.3.2 ViDIR Group

Data from the ViDIR Group were accessed and analyzed following ethics committee permission (Protocol-No. 1804/2017) at the Medical University of Vienna.

- Reliable Diapositives (ViDIR Legacy): Dermatoscopic pictures had to be preserved as diapositives acquired with analog cameras before the introduction of digital cameras. These images were shot via the Heine Dermaphot system, and for the sake of study and preservation, both immersion fluid

and physical copies were generated utilizing the E-6 procedure.

- Currently Available Material (ViDIR Current): Since 2005, we've been documenting digital dermatoscopic pictures with a DermLite™ FOTO system and archiving images and meta-data in a central database which means single cases along with the Heine of Delta 20. Images of the same lesion obtained at various magnifications are included in this set for demonstrate local patterns and features.
- MoMax (ViDIR MoleMax): High-risk patients who underwent surgery to remove early melanoma were given digital dermatoscopic follow-up examinations, which resulted in less removal of melanocytes. Follow-up appointments are scheduled every six to twelve months on average. The MoleMax HD System has been used since 2015 to collect digital dermatoscopic images (Derma Medical Systems, Vienna). The majority of patients were found to have an excessive number of nevi.

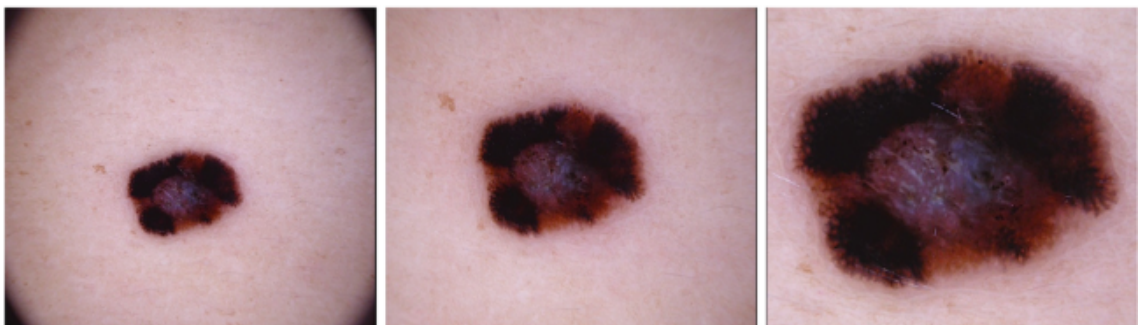


*Figure 9 :Instead of cropping a large source photo, the original photos had three different magnifications and viewpoints.*

### 3.4 Technical Validation

As a response to a request for assistance with manual adjustments to the histogram that would make it easier for human viewers to access the information, expert dermatologists were contacted. Only photos that are overexposed and those that have a visible tone that changes the natural skin tone of the image need to be edited. In order to evaluate the accuracy of the brightness color projections after the correction, the gray-world assumption was utilized. The gray-world assumption is a method of picture white-balancing that operates under the presumption that the majority of the image in question is comprised of a color that is neutral gray. When comparing images taken before and after changes to the historiography, this makes it possible to illustrate the difference in image clarity with a straightforward graph depicting the average color of the image.

# Chapter 4

## Dataset

### 4.1 Required Libraries

In order to make a working CNN model various libraries need to be installed in the virtual environment and further imported in our notebook code. The primary library is tensorflow which is used as backend for this notebook. Other libraries used are as follows

- Numpy
- PIL
- Keras
- Sklearn
- Pandas
- Matplotlib

### 4.2 Data Cleaning

The HAM10000 metadata file has null values in the “age” column. These null values are filled with the mean age value of the whole dataset using the “.fillna()” function with inplace parameters set to true.

### 4.3 Exploratory Data Analysis

Our utilized dataset contains additional information, such as the localization and diagnosis of skin growths. Also includes information on the gender and age of afflicted individuals.

### 4.3.1 Distribution of Type of Cancer

Figure 10 shows the distribution of the number of images in seven different categories of lesions. The given figure shows that melanocytic nevi has the most number of images.

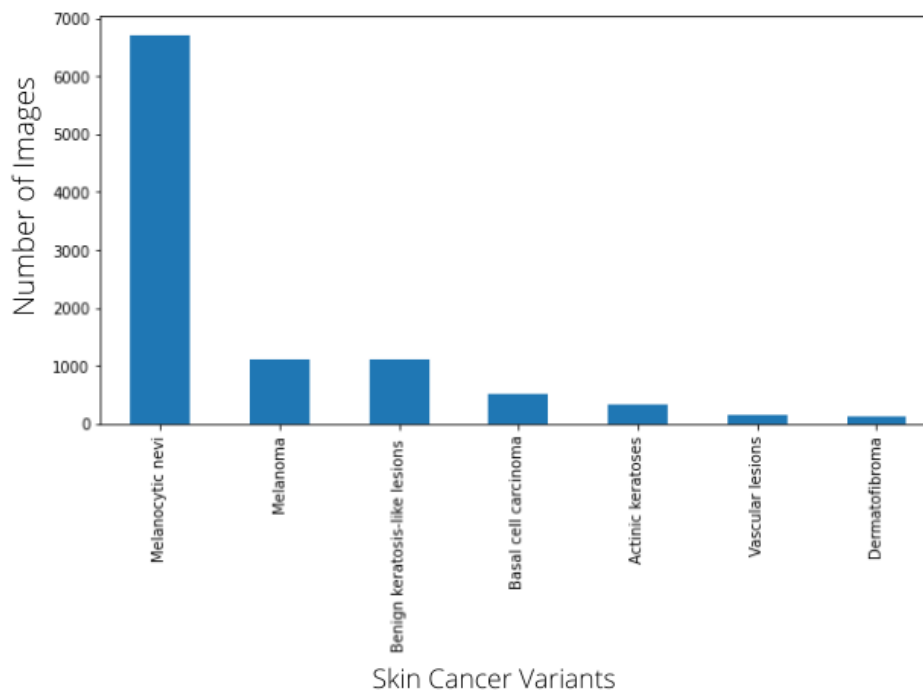


Figure 10 : Distribution of types of skin cancer

### 4.3.2 Distribution with Diagnosis Type

The types of diagnosis that were maintained to confirm the type of lesion in the image are Histopathy, Follow-up examination, expert consensus or confocal microscopy. Almost 50 percent of the images were confirmed through histopathy figure[11] shows.

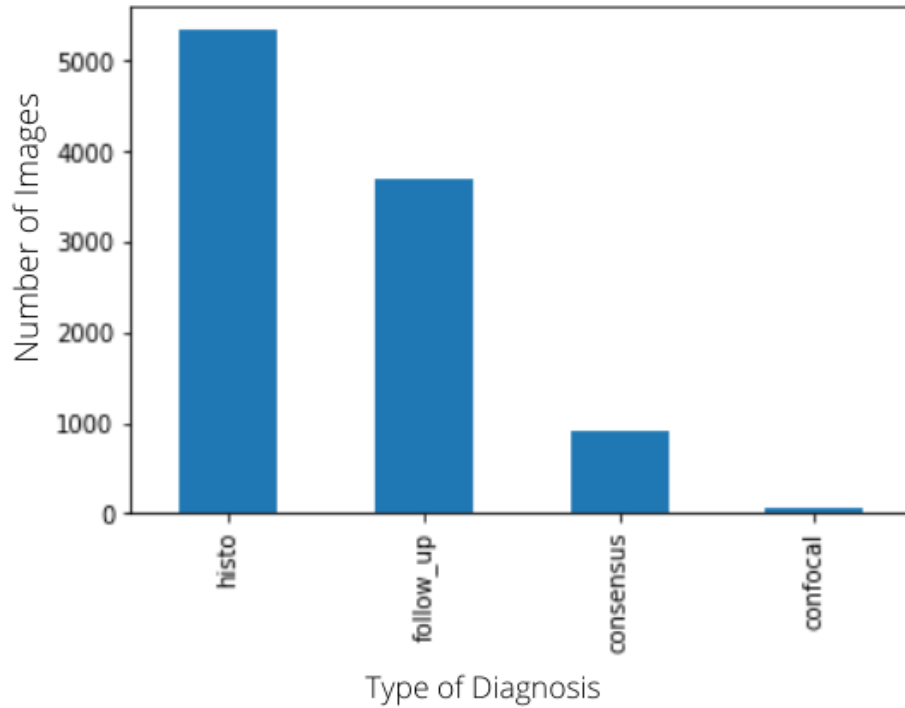


Figure 11: Diagnosis Type

### 4.3.3 Distribution with Localization

The following figure [12] demonstrates the distribution of the lesions according to the part of the body they were in. Most of the lesions were on the back or lower-extremity.

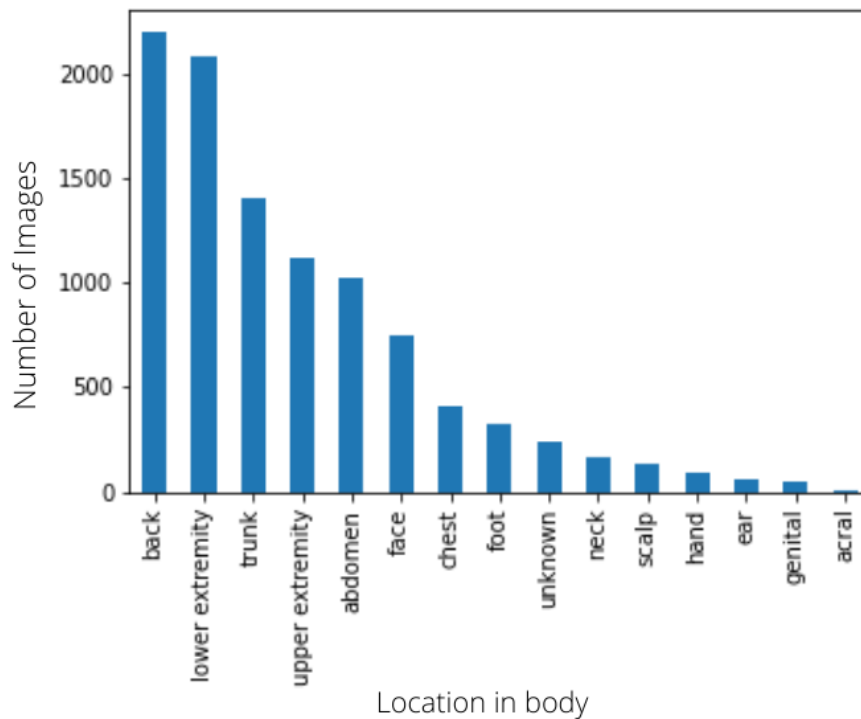
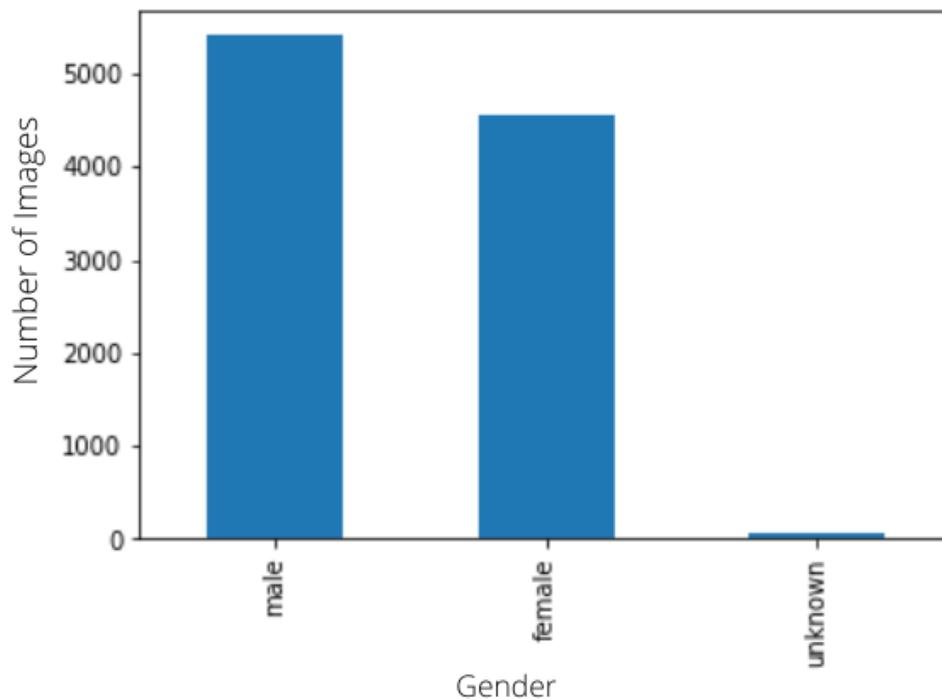


Figure 12: Localization



### 4.3.4 Distribution with Gender

The Figure 13 shows the number of men , women and unspecified gendered participants that gave their lesion's image data for the HAM10000 dataset. It also helps to identify the biasness that our models might have due to the gender ratio in the data.



*Figure 13: Gender Distribution*

### 4.3.5 Distribution with Age

Most of the image data were of participants that aged in the range of 40-70. The Figure[11] shows the whole spectrum of data that has been collected over the range of ages which will help to restructure any conclusion regarding any relation to age with the lesions.

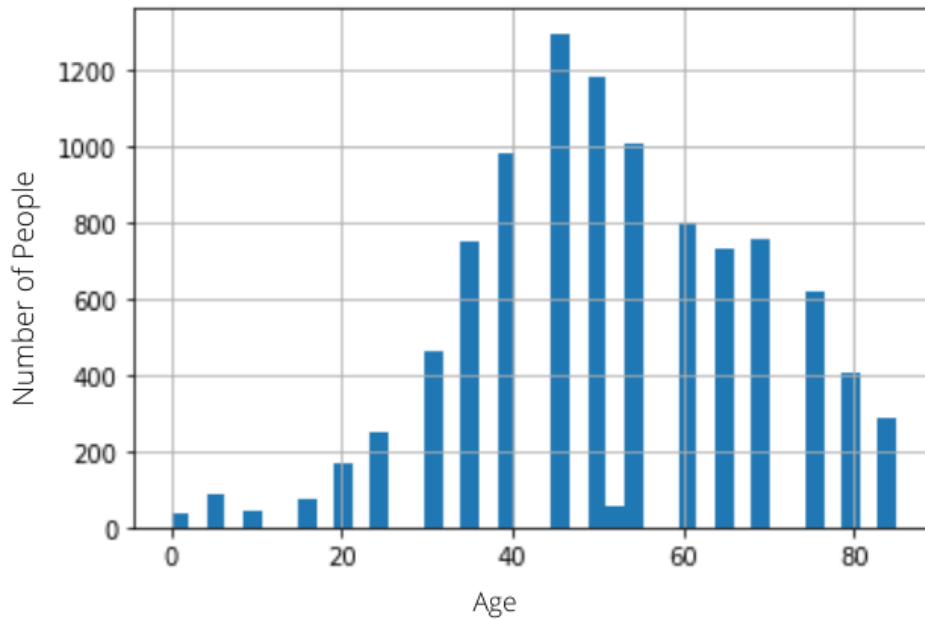


Figure 14: Age Distribution

### 4.3.6 Scatter-plot Diagram of Distribution of Age Against Distribution of Cancer

The scatterplot data projection Figure[15] of each type of lesion and the age when it was diagnosed. Therefore we can identify which sort of lesions start to develop at which stage of life. Consecutively, people can be made aware and testing could be started sooner accordingly.

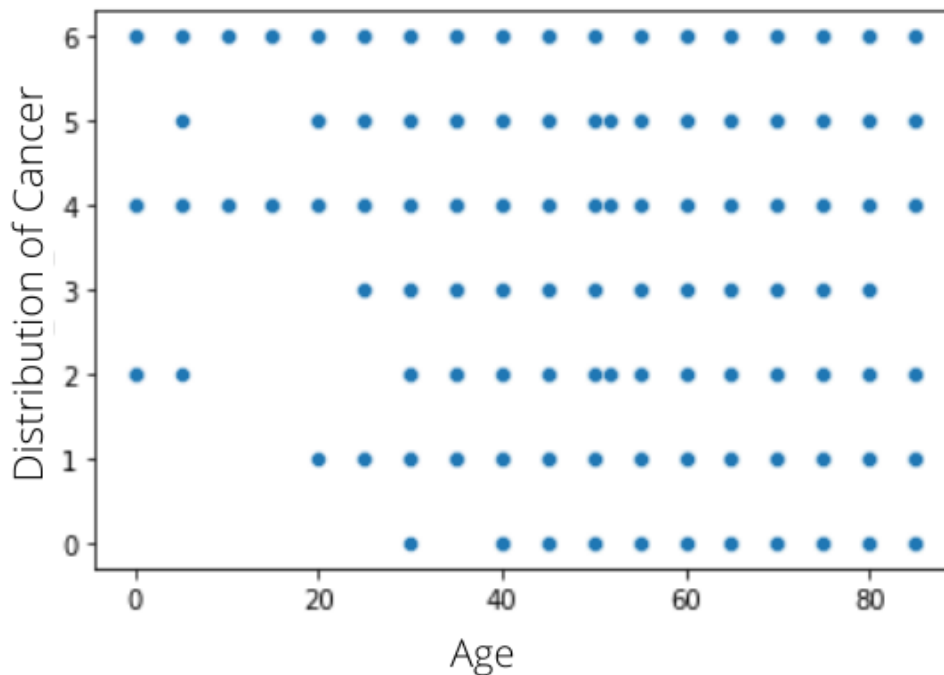


Figure 15: Scatter Plot

# Chapter 5

## Data Augmentation

As deep networks require a great amount of data to achieve high accuracy, data augmentation is essential. We see that the data has a large class imbalance. We believe we can improve our data to solve this gap. We must artificially boost our HAM 10000 dataset[16] to prevent the difficulties caused by over-fitting. The amount of our present dataset may be greatly expanded. The aim is to make modest adjustments to the preparations to imitate the variances. Many basic augmentations, such as scaling, splitting, shearing and zooming are only a handful of the many options.

- The photos were rotated at random angles ranging from 0 to 20 degrees, after which the blank portions were needed to be filled.
- The fill mode option has a default value of "nearest," which populates the empty space with the pixel values that are the closest to each other.
- We can also shear, zoom and shift (width and height) the images up to 20% at random.
- We've also adjusted the images vertically and horizontally to deal with the fact that images input to the model aren't always centered.

### 5.1 Reading and Processing the Data

We used the pandas library in order to read the metadata and saved it as a data frame. A column named "path" is made for every image location. This column will be used for loading and resizing the images. Moreover two more column has been made named as "cell\_type" and "cell\_type\_idx". In the "cell\_type" column we have stored the type of skin lesion and in "cell\_type\_idx" we have stored cell type index.

### 5.1.1 Loading and Resizing

TensorFlow seems unable to deal directly with the dataset's images although they are much larger ( $450 \times 600 \times 3$ ) than it can accommodate. As a consequence of this, the combined colored pixel data from the provided CSV file inside the dataset was utilized for our model, and the photographs that were provided were reduced in size to  $224 \times 224$ . Using the path we opened image by the help of PIL library. Afterward the image is resized into  $224 \times 224$  pixels from  $450 \times 600$  and stored in a cell named images using the numpy array. Both loading and resizing is done using the Lamda function which acts as an iterative loop.

## 5.2 Train-Test Split

The dataset is divided into training, testing, and validation portions. This is a standardized approach to data science. The training dataset is the basis for every CNN algorithm, serving as an example of how sophisticated technology like neural networks may be utilized to learn and create more complicated results. It includes not just the facts but also an estimate of the production that is anticipated. The training dataset provides “ground truth” information to our algorithms. Nevertheless, the test dataset is utilised to quantify how the preparation dataset was utilized to develop our program. Since the analysis would almost surely “know” the predicted conclusion if we just repeated the training dataset during the testing process, which would defeat the purpose of evaluating the approach.

## 5.3 Normalization

When the images of the dataset were resized and converted into a numpy array, the numbers ranged from 0 to 255 as pixel data. However, these values are not processed by the neural networks therefore the values have to turned to a floating value from 0 to 1. For this reason, the pixel data is subtracted by the mean value and divided by the standard deviation of the values. This process is used to set the `x_train` and the `x_test` sets.

### 5.3.1 Label-Encoding

Here on labels, there are seven distinct classes of skin cancer categories, ranging from 0 to 6. This is used as `y_train` data to fit the model. The encoding for data categorization purposes is as follows:

Label Name	akiec	bcc	bkl	df	mel	nv	vasc
Index Value	0	1	2	3	4	5	6

Table 5.1: Label encoding for 7 categories.

### 5.3.2 Splitting Training and Validation Split

A relatively small percentage, twenty percent, of the data from the training set was used to verify the model, while the remaining eighty percent was employed to train the model. Utilizing a validation dataset helps avoid models from being over-fit to the data. Using this data set, we are not adjusting the network's weights; rather, we are checking to make sure that any gain in accuracy over the train set is a genuine gain over data that the network. If the train set's accuracy improves while the validation set's quality drops, the neural network is overfit and training should stop.

# Chapter 6

## Model Building

### 6.1 Work Plan

The goal of our model is to compare the basic CNN models with the merged concatenated models depending on the efficiency, accuracy and loss value in deducing the type of skin disease in the provided image and predicting precisely among as many as seven types of diseases for now. In order to achieve success across these many types of skin diseases, we divide our dataset into a training set, validation set, and test set, where the training set uses 80%, validation uses 10% and test uses 10% of the dataset. The training and validation sets are augmented to get more images as the dataset is limited. The augmented datasets are then run through the tuned model to train it. After training is completed, a few sample pictures with a known disease label are used as the test set. The model's prediction and accuracy of the prediction are then calculated. Learning rate and other various tuning are done along the way to find maximum accuracy.

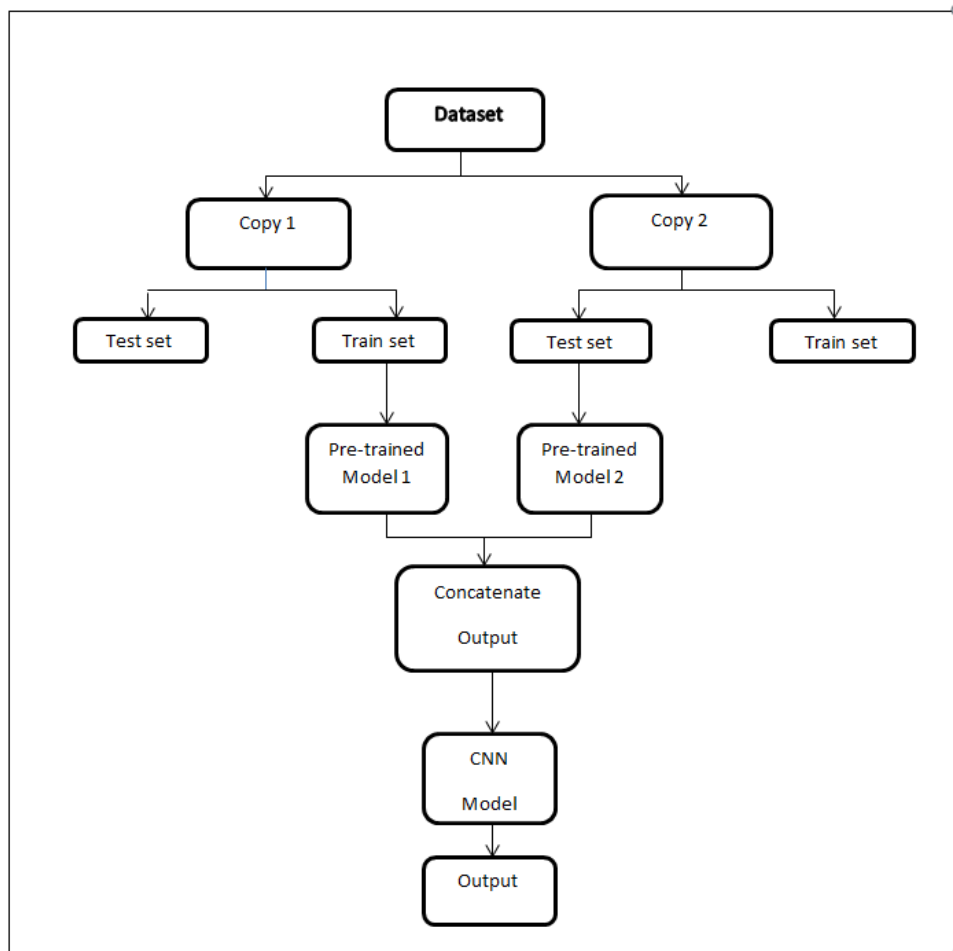


*Figure 16 :The figure above gives a simplified representation on how the whole process works.*

## 6.2 Our Model and Initial Iteration

At the very beginning we made a prototype as our first attempt at detecting skin disease of 7 different categories using image datasets. Using transfer learning and fine-tuning using Keras applications, we have used several pre-trained models on ImageNet. ImageNet is an image database organized according to the WordNet hierarchy (currently only the nouns), in which hundreds and thousands of images depict each node of the hierarchy. The project has been instrumental in advancing computer vision and deep learning research. The data is available for free to researchers for non-commercial use. The ImageNet dataset is a vast collection of human-annotated photographs designed by academics for developing computer vision algorithms. The past work was done on much smaller dataset.

With the HAM10000 dataset our input size has significantly increased but the number of categories of data has decreased. Now we have run our model on 7 different categories using single as well as multi pre-trained CNN models via transfer learning. We use 3 dense layers with 512 neurons each along with Flatten, Dropout and BatchNormalization layers to provide efficient and smooth transition of data between the layers. Lastly, the dense layer with seven neurons as per the categories with activation “softmax” is added for categorical classification of the input data.

We have used transfer learning either with one pre-trained model or two. The models where we have used one pre-trained model such as Vgg16, we have frozen the last fully connected layer and made all the layers untrainable. After that, we transferred the output to one of our dense layers. On the other hand, when we used transfer learning with two pretrained models. We fed a copy of our dataset into both the models and froze the fully connected layer and made all the layers non-trainable. Then the output of both the pre-trained model is concatenated and passed to the dense layer. With the help of the pretrained models, we have tried to find the best model to use in determining skin cancer across 7 different categories.



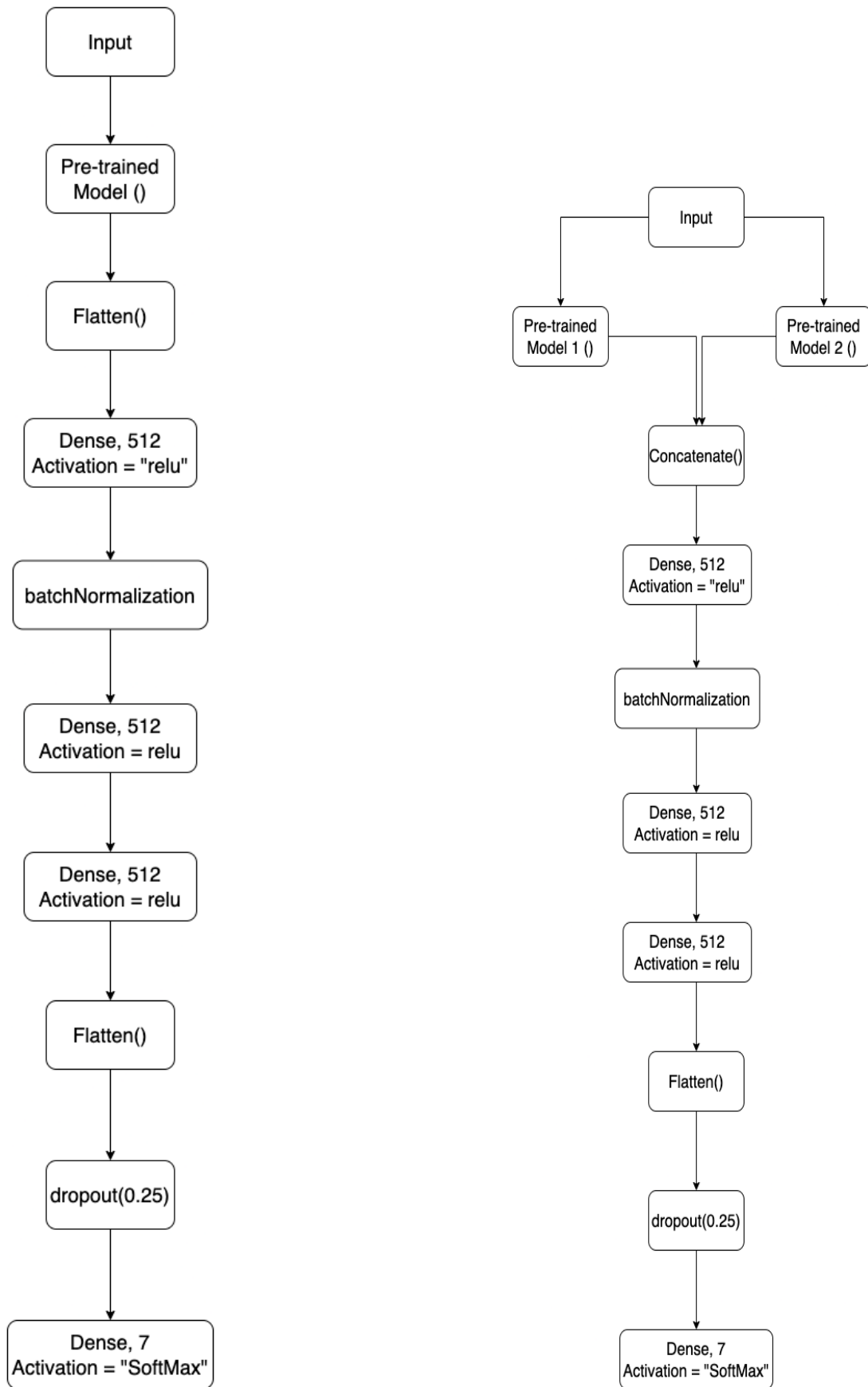


Figure16:Our Model

# Chapter 7

## Model Evaluation and Result Analysis

### 7.1 Annealing

After adding layers to the model, we must configure a score function, a loss function, and an optimisation technique. We define the loss function to quantify how poorly our model performs on labeled images. It is the rate of error between observed and expected labels. For categorical classifications, we utilize a particular form called "categorical\_crossentropy." Optimizer is the most essential function. This function iteratively optimizes settings to minimize loss. We chose the Adam optimizer because it combines the benefits of two previous stochastic gradient descent improvements. The annealer monitors the validation accuracy. If the validation does not improve for three consecutive epochs then the learning rate value is decreased by half. The starting learning rate value is 0.01.

### 7.2 Fitting Model

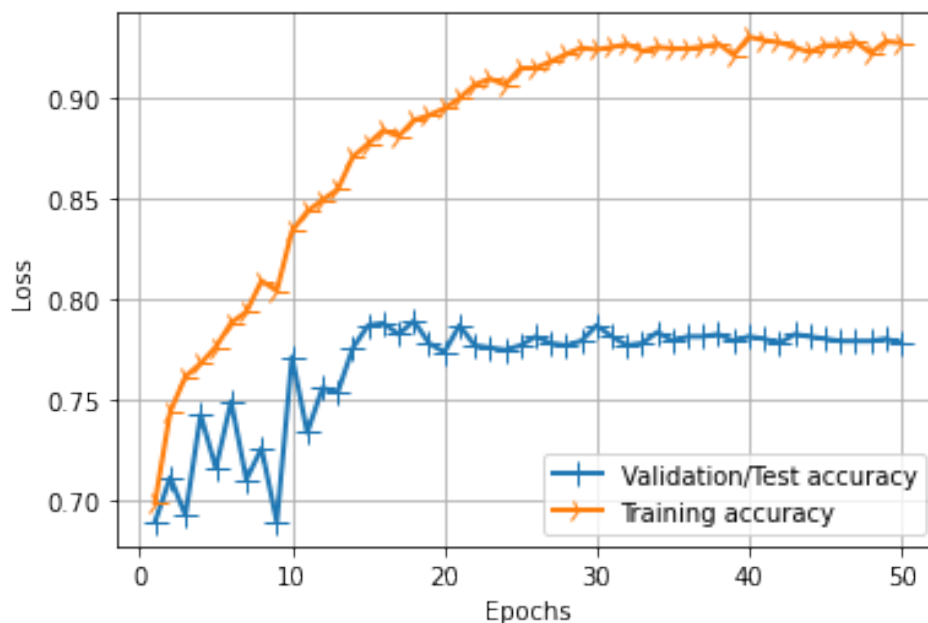
The model is fitted into the `x_train` (carries the images) and `y_train` (carries all labels) using `model.fit()` function. The function is called by passing the parameters `x_train`, `y_train`, `batch_size` that were kept at 64 for all of our model training. Validation data = `x_validate`, `y_validate`. Steps per epoch for both train and validation were calculated by the number of images in that particular set divided by batch size.

## 7.3 Transfer Learning Using One Pre-trained Model

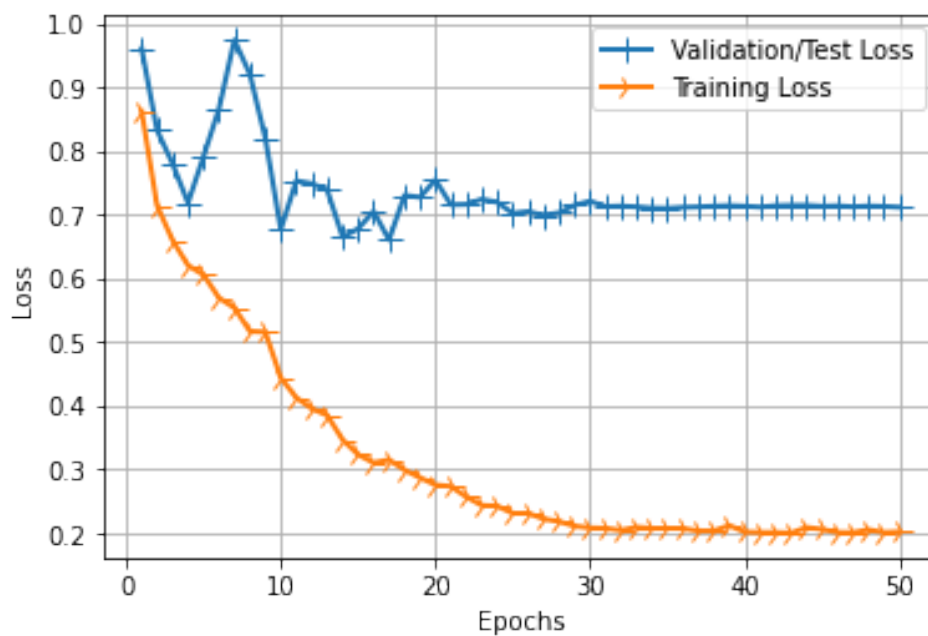
### 7.3.1 Transfer Learning with VGG-16

	Train	Validation	Test
Accuracy	92.73%	77.83%	79.24%
Loss	0.2016	0.7113	0.6929

Table 7.1: Results of VGG16



*Accuracy of VGG16*

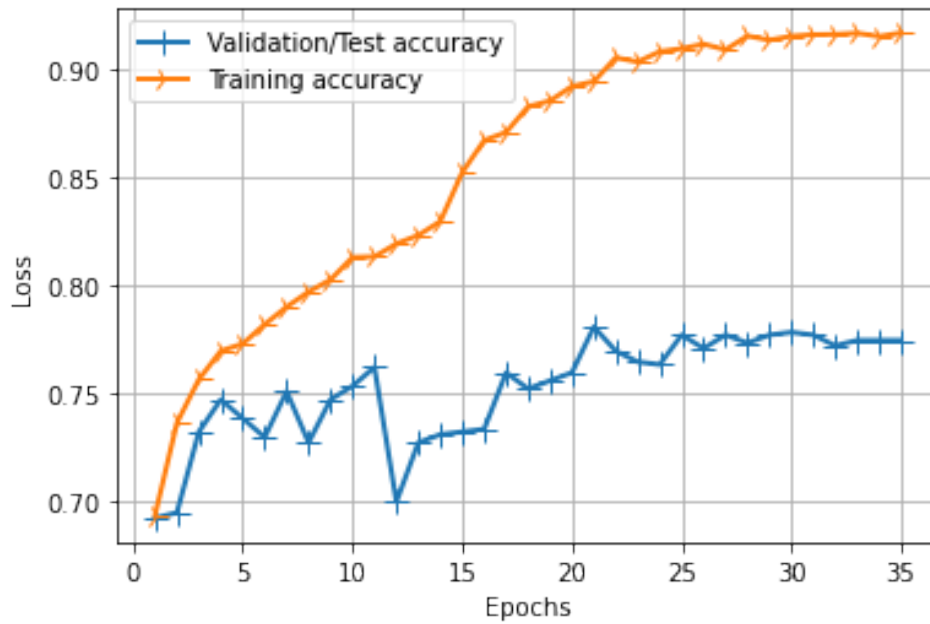


*Loss of VGG16*

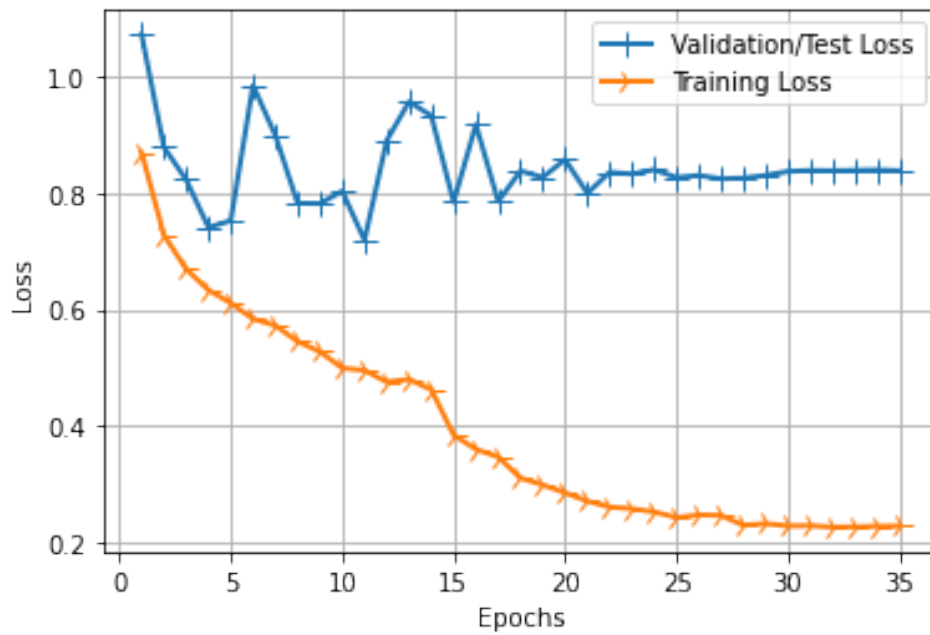
### 7.3.2 Transfer Learning with VGG19

	Train	Validation	Test
Accuracy	88.06%	78.05%	77.45%
Loss	0.3069	0.6695	0.7061

Table 7.2: Results of VGG19



*accuracy of VGG19*

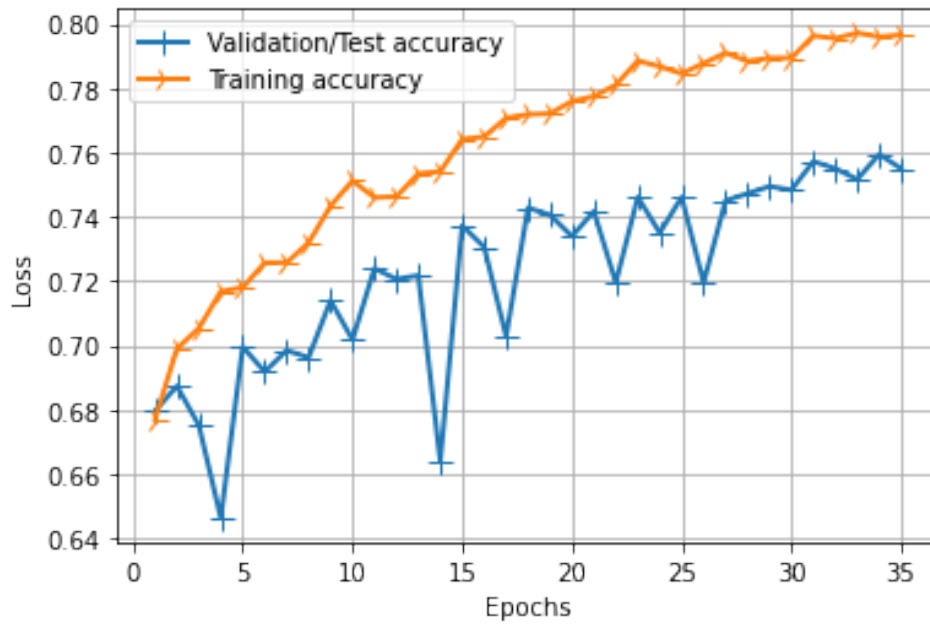


*Loss of VGG19*

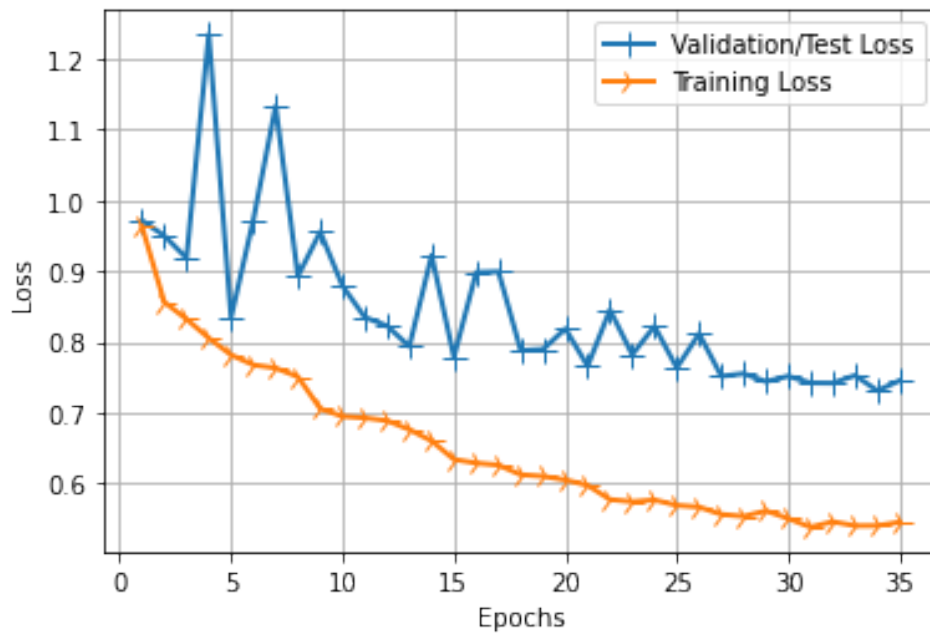
### 7.3.3 Transfer Learning with ResNet50

	Train	Validation	Test
Accuracy	79.66%	75.50%	74.65%
Loss	0.5457	0.7456	0.7809

Table 7.3: Results of ResNet50



*Accuracy of ResNet50*

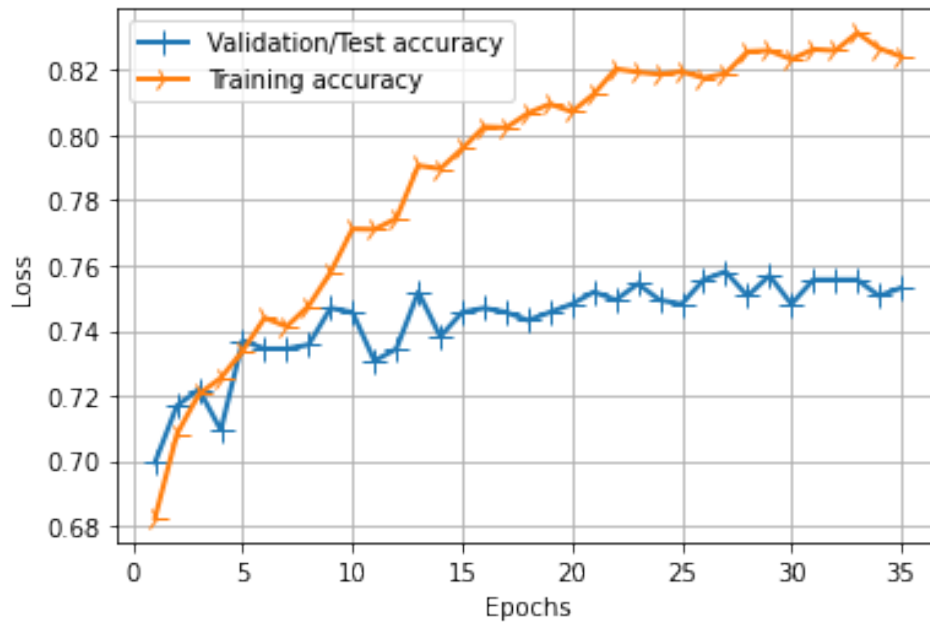


*Loss of ResNet50*

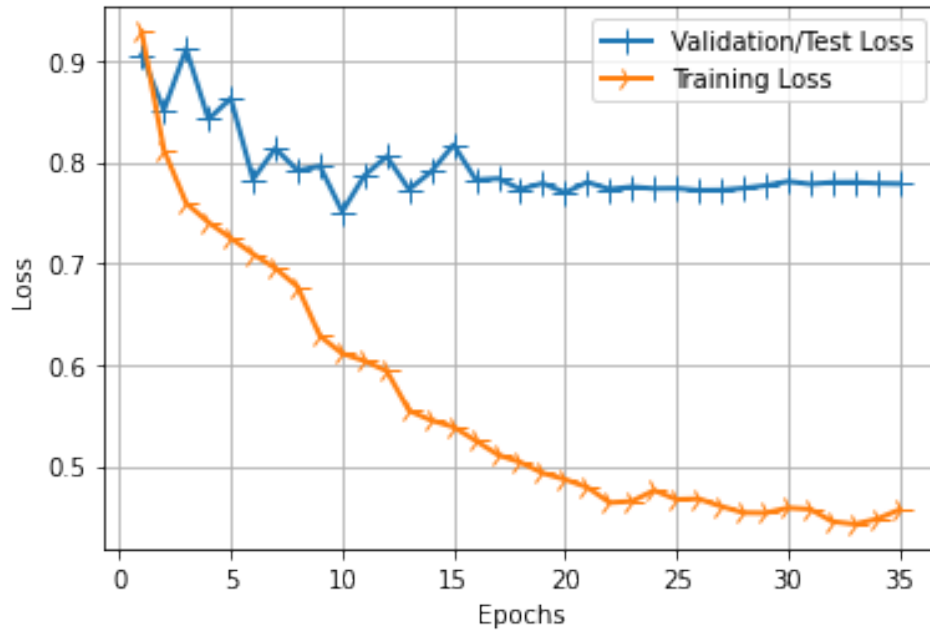
### 7.3.4 Transfer Learning with InceptionV3

	Train	Validation	Test
Accuracy	82.41%	75.31%	73.34%
Loss	0.4568	0.7783	0.7935

Table 7.4: Results of InceptionV3



*Accuracy InceptionV3*



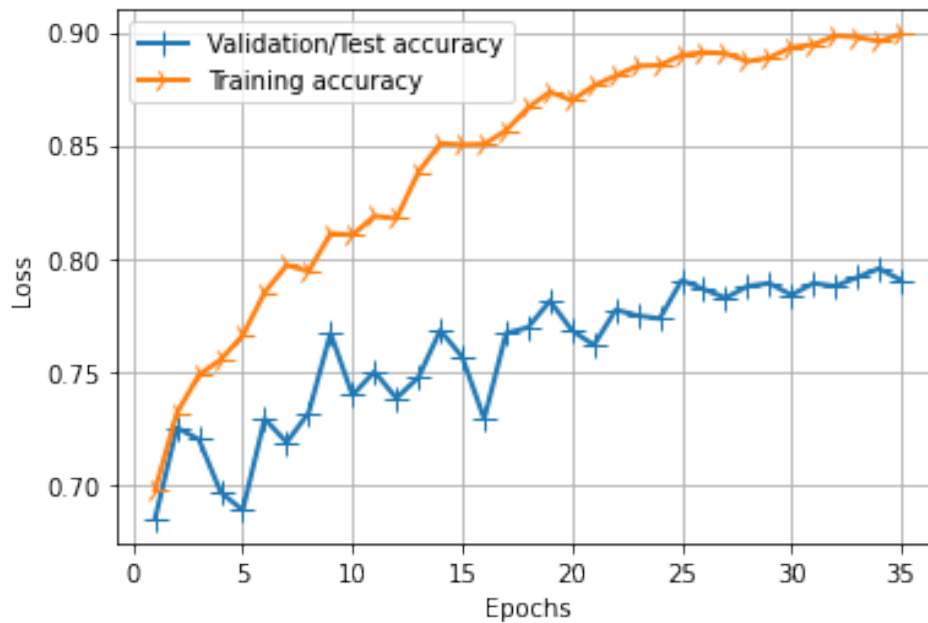
*Loss InceptionV3*

## 7.4 Transfer Learning with Merged Models

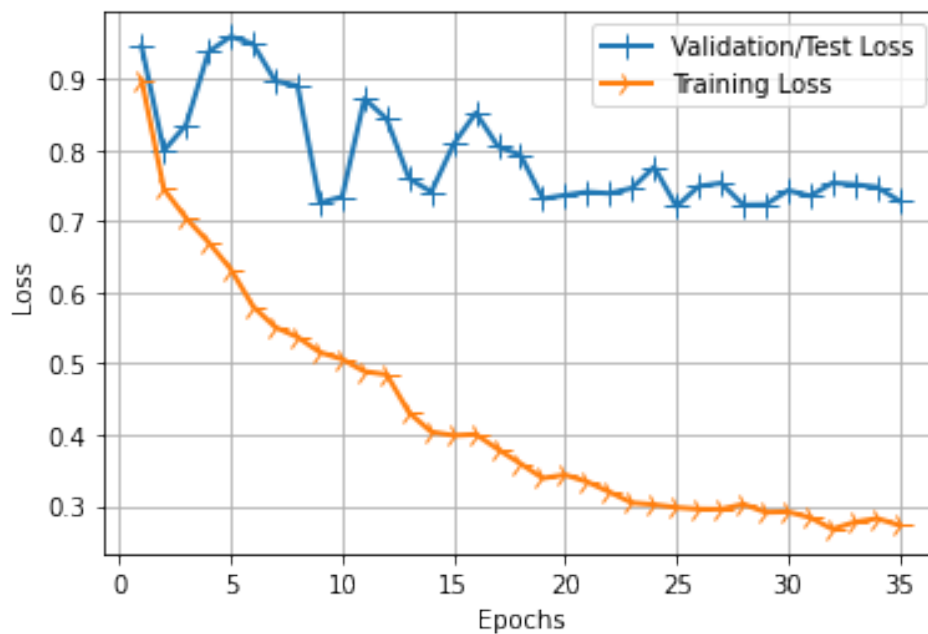
### 7.4.1 Transfer Learning with ResNet50 and VGG19

	Train	Validation	Test
Accuracy	89.92%	79.04%	78.32%
Loss	0.2726	0.7284	0.7313

Table 7.5: Results of concatenated ResNet50 and VGG19 model



*Accuracy of ResNet50 and VGG19*

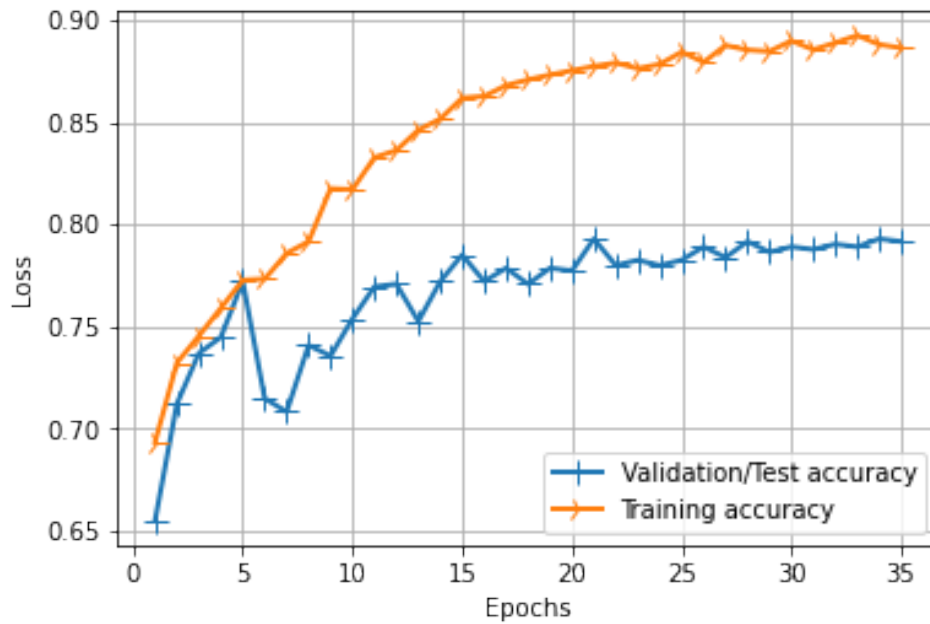


*Loss of ResNet50 and VGG19*

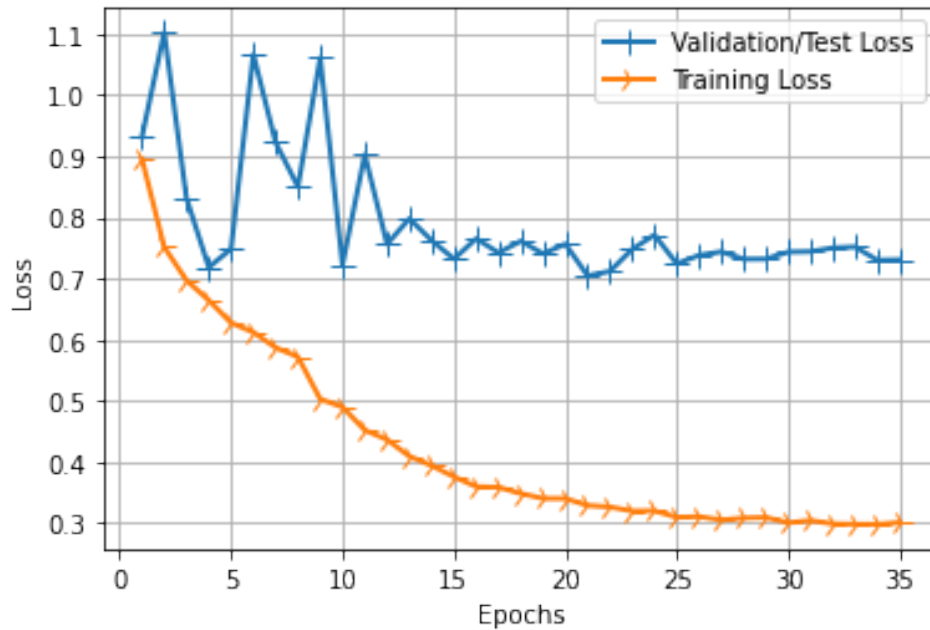
## 7.4.2 Transfer Learning with ResNet50 and VGG16

	Train	Validation	Test
Accuracy	88.64%	79.17%	79.63%
Loss	0.3011	0.7306	0.7863

Table 7.6: Results of concatenated ResNet50 and VGG16 model



*Accuracy of VGG16 ResNet50*



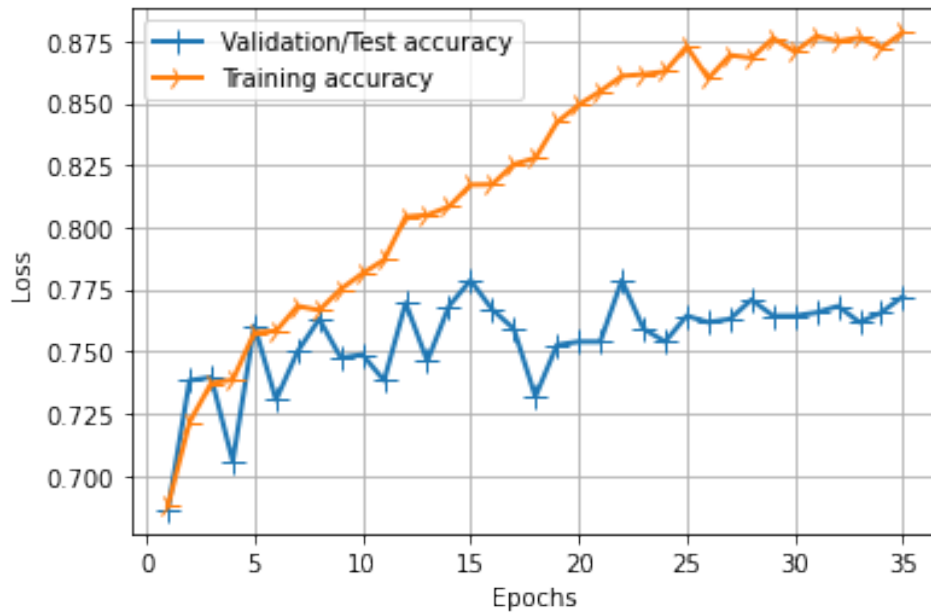
*Loss of VGG16 ResNet50*



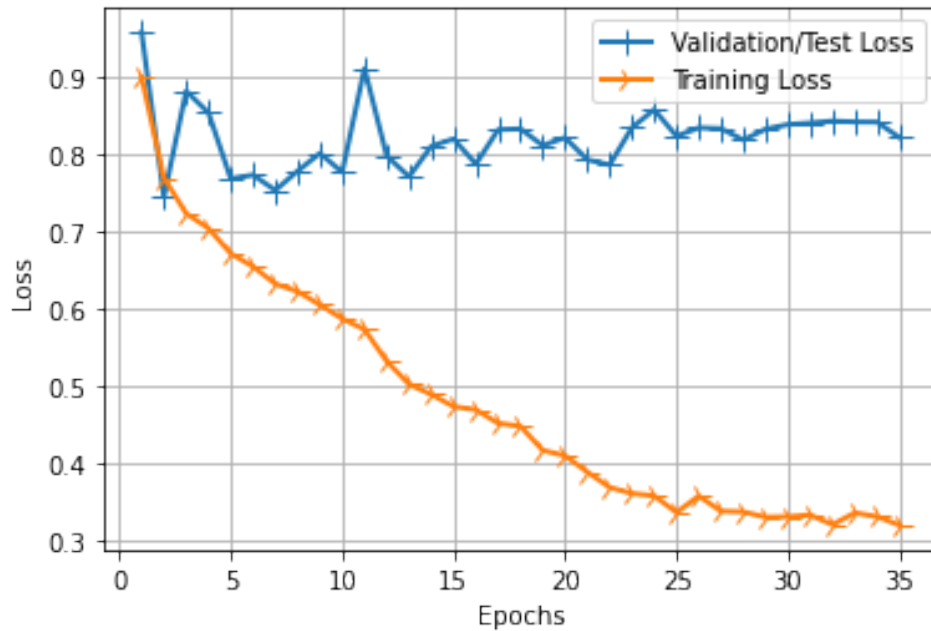
### 7.4.3 Transfer Learning with ResNet50 and InceptionV3

	Train	Validation	Test
Accuracy	87.85%	76.31%	75.19%
Loss	0.3193	0.8371	0.7983

Table 7.7: Results of concatenated ResNet50 and InceptionV3 model



*Accuracy of ResNet50 and InceptionV3*

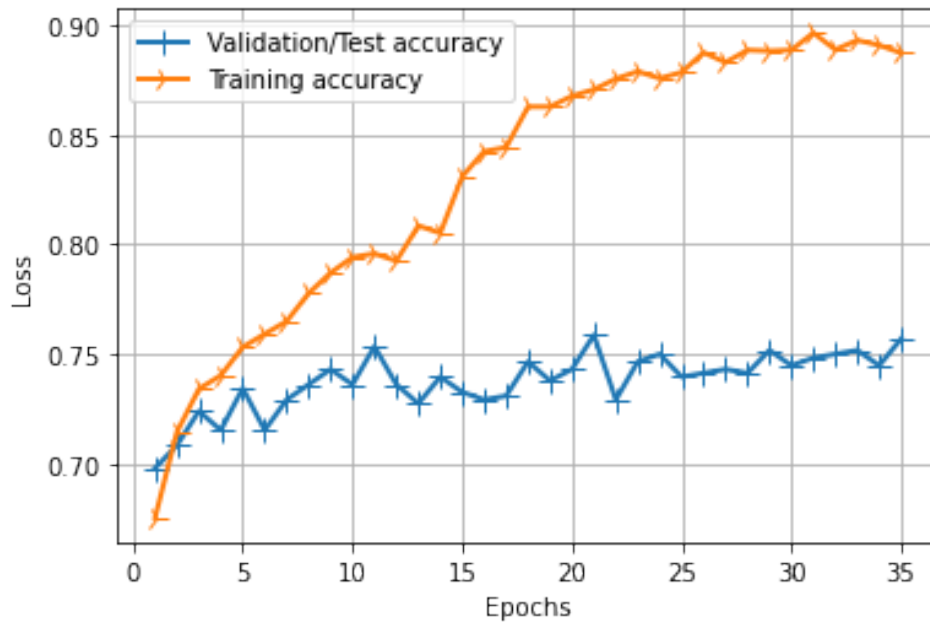


*Loss of ResNet50 and InceptionV3*

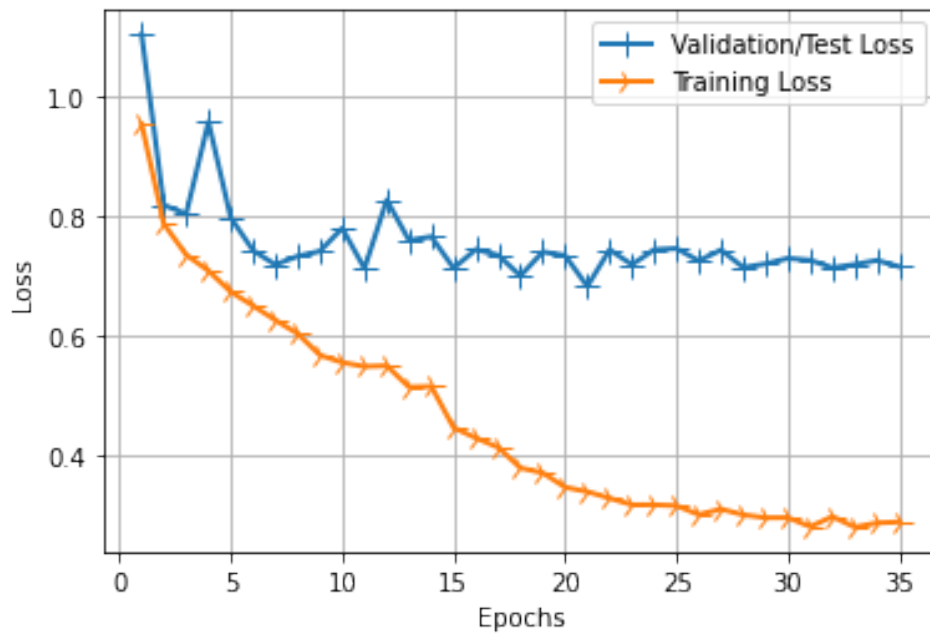
### 7.4.4 Transfer Learning with VGG16 and InceptionV3

	Train	Validation	Test
Accuracy	88.74%	75.69%	75.89%
Loss	0.873	0.7155	0.7826

Table 7.8: Results of concatenated VGG16 and InceptionV3 model



*Accuracy of VGG16 and InceptionV3*

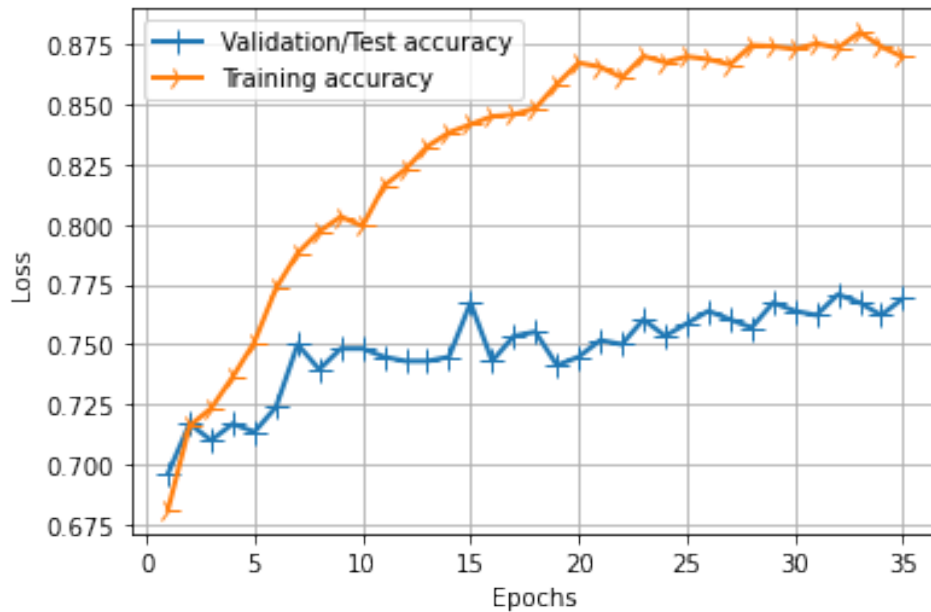


*Loss of VGG16 and InceptionV3*

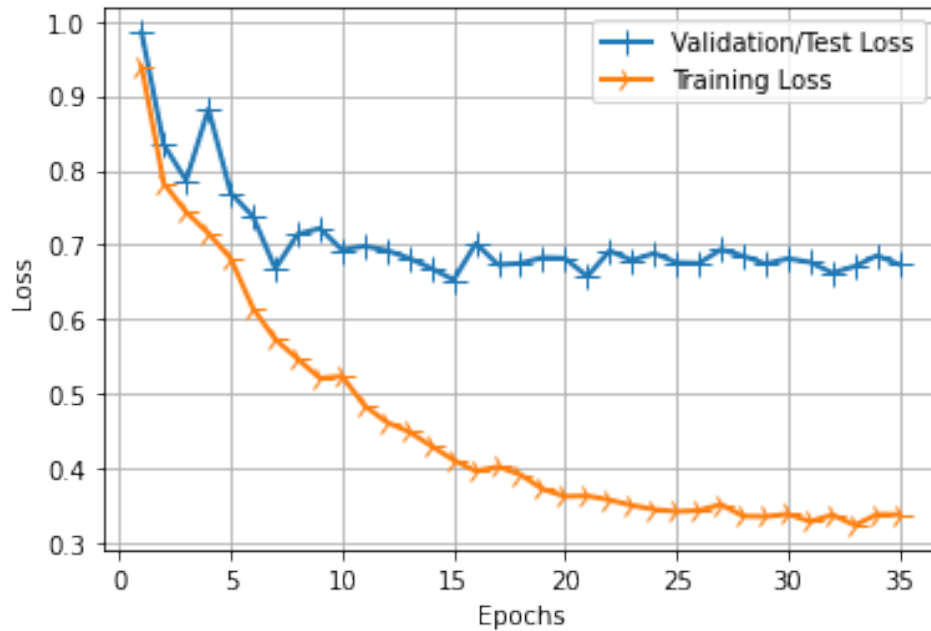
### 7.4.5 Transfer Learning with VGG19 and InceptionV3

	Train	Validation	Test
Accuracy	86.96%	77.91%	76.15%
Loss	0.3383	0.6737	0.6632

Table 7.9: Results of concatenated VGG19 and InceptionV3 model



*Accuracy of VGG19 and InceptionV3*



*Loss of VGG19 and InceptionV3*

## 7.5 Analysis and Comparison of the Models

Models	Test Accuracy	Test Loss
VGG19	77.45%	0.7061
VGG16	79.24%	0.6929
ResNet50	74.65%	0.7809
InceptionV3	73.34%	0.7935
VGG19 + ResNet50	78.32%	0.7313
VGG19 + InceptionV3	76.15%	<b>0.6632</b>
VGG16 + ResNet50	<b>79.63%</b>	0.6863
VGG16 + InceptionV3	75.89%	0.7826
ResNet50 + InceptionV3	75.19%	0.7983

Table 7.10: Test Accuracy and Loss comparisons of all models

The table above shows the test accuracy of all models run on the same dataset with the same dense layers containing the same number of neurons. The hyper-parameters are kept the same as well as the batch size and image sizes. The coherence of all the variables are maintained in order to test every single pre-trained and merged pre-trained models on a level playing field. The highest test accuracy was obtained using the VGG16 ResNet50 merged models. However, the lower test loss value was achieved by VGG19 InceptionV3. The merged models took longer time to train, almost a minute longer than the single models.

# Chapter 8

## Conclusion

The goal of our research was to find a comprehensive data with different methods of transfer learning and training between four renowned CNN models. With a specific set parameter and conditions we have found two of the merged models to give slightly better results in terms of test accuracy and loss. The research was tied to certain constraints due to shortage of diversified data as well as to provide and fairness between the models. Therefore, it is not concluded that a different set of parameters, architecture, data processing method and other variables would still provide the same model/models to give the best result.

However, this research may open paths to new comparison and analysis research between models to achieve greater results and standards not only in the field of image processing but also other fields that require CNN and machine learning. With the progress of better classification between these models we hope to achieve a model where the results can be reliable enough so that doctors and medical facilities can implement the model in aiding real-world applications and help ease human effort and difficulty.

# Bibliography

- [1] M. Binder, A. Steiner, M. Schwarz, S. Knollmayer, K. Wolff, and H. Pehamberger, “Application of an artificial neural network in epiluminescence microscopy pattern analysis of pigmented skin lesions: A pilot study,” en, *British Journal of Dermatology*, vol. 130, no. 4, pp. 460–465, Apr. 1994, ISSN: 0007-0963, 1365-2133. DOI: 10.1111/j.1365-2133.1994.tb03378.x. [Online]. Available: <https://onlinelibrary.wiley.com/doi/10.1111/j.1365-2133.1994.tb03378.x> (visited on 05/22/2022).
- [2] —, “Application of an artificial neural network in epiluminescence microscopy pattern analysis of pigmented skin lesions: A pilot study,” en, *British Journal of Dermatology*, vol. 130, no. 4, pp. 460–465, Apr. 1994, ISSN: 0007-0963, 1365-2133. DOI: 10.1111/j.1365-2133.1994.tb03378.x. [Online]. Available: <https://onlinelibrary.wiley.com/doi/10.1111/j.1365-2133.1994.tb03378.x> (visited on 05/22/2022).
- [3] T. Gansler, P. A. Ganz, M. Grant, *et al.*, “Sixty Years of CA: A Cancer Journal for Clinicians,” en, *CA: A Cancer Journal for Clinicians*, vol. 60, no. 6, pp. 345–350, Nov. 2010, ISSN: 0007-9235. DOI: 10.3322/caac.20088. [Online]. Available: <http://doi.wiley.com/10.3322/caac.20088> (visited on 05/22/2022).
- [4] R. S. Stern, “Prevalence of a history of skin cancer in 2007: Results of an incidence-based model,” eng, *Archives of Dermatology*, vol. 146, no. 3, pp. 279–282, Mar. 2010, ISSN: 1538-3652. DOI: 10.1001/archdermatol.2010.4.
- [5] “35th Annual International Conference of the IEEE Engineering in Medicine and Biology Society,” *IEEE Pulse*, vol. 4, no. 3, pp. 41–41, May 2013, ISSN: 2154-2287. DOI: 10.1109/MPUL.2013.2257519. [Online]. Available: <http://ieeexplore.ieee.org/document/6518246/> (visited on 05/22/2022).
- [6] A. N. Hoshyar, A. Al-Jumaily, and A. N. Hoshyar, “The Beneficial Techniques in Preprocessing Step of Skin Cancer Detection System Comparing,” en, *Procedia Computer Science*, vol. 42, pp. 25–31, 2014, ISSN: 18770509. DOI: 10.1016/j.procs.2014.11.029. [Online]. Available: <https://linkinghub.elsevier.com/retrieve/pii/S1877050914014677> (visited on 05/22/2022).
- [7] S. Jain, V. Jagtap, and N. Pise, “Computer Aided Melanoma Skin Cancer Detection Using Image Processing,” en, *Procedia Computer Science*, vol. 48, pp. 735–740, 2015, ISSN: 18770509. DOI: 10.1016/j.procs.2015.04.209. [Online]. Available: <https://linkinghub.elsevier.com/retrieve/pii/S1877050915007188> (visited on 05/22/2022).

- [8] H. W. Rogers, M. A. Weinstock, S. R. Feldman, and B. M. Coldiron, “Incidence Estimate of Nonmelanoma Skin Cancer (Keratinocyte Carcinomas) in the U.S. Population, 2012,” eng, *JAMA dermatology*, vol. 151, no. 10, pp. 1081–1086, Oct. 2015, ISSN: 2168-6084. DOI: 10.1001/jamadermatol.2015.1187.
- [9] C. Szegedy, V. Vanhoucke, S. Ioffe, J. Shlens, and Z. Wojna, “Rethinking the Inception Architecture for Computer Vision,” *arXiv:1512.00567 [cs]*, Dec. 2015, arXiv: 1512.00567. [Online]. Available: <http://arxiv.org/abs/1512.00567> (visited on 05/22/2022).
- [10] A. Esteva, B. Kuprel, R. A. Novoa, *et al.*, “Dermatologist-level classification of skin cancer with deep neural networks,” en, *Nature*, vol. 542, no. 7639, pp. 115–118, Feb. 2017, ISSN: 0028-0836, 1476-4687. DOI: 10.1038/nature21056. [Online]. Available: <http://www.nature.com/articles/nature21056> (visited on 05/22/2022).
- [11] R. H. Fletcher, “Colonoscopy outreach increased CRC screening more than FIT outreach; both were better than usual care,” en, *Annals of Internal Medicine*, vol. 167, no. 12, JC65, Dec. 2017, ISSN: 0003-4819. DOI: 10.7326/ACPJC-2017-167-12-065. [Online]. Available: <http://annals.org/article.aspx?doi=10.7326/ACPJC-2017-167-12-065> (visited on 05/22/2022).
- [12] C. Karimkhani, R. P. Dellavalle, L. E. Coffeng, *et al.*, “Global Skin Disease Morbidity and Mortality: An Update From the Global Burden of Disease Study 2013,” en, *JAMA Dermatology*, vol. 153, no. 5, p. 406, May 2017, ISSN: 2168-6068. DOI: 10.1001/jamadermatol.2016.5538. [Online]. Available: <http://archderm.jamanetwork.com/article.aspx?doi=10.1001/jamadermatol.2016.5538> (visited on 05/22/2022).
- [13] J. G. Muzic, A. R. Schmitt, A. C. Wright, *et al.*, “Incidence and Trends of Basal Cell Carcinoma and Cutaneous Squamous Cell Carcinoma,” en, *Mayo Clinic Proceedings*, vol. 92, no. 6, pp. 890–898, Jun. 2017, ISSN: 00256196. DOI: 10.1016/j.mayocp.2017.02.015. [Online]. Available: <https://linkinghub.elsevier.com/retrieve/pii/S0025619617301647> (visited on 05/22/2022).
- [14] U.-O. Dorj, K.-K. Lee, J.-Y. Choi, and M. Lee, “The skin cancer classification using deep convolutional neural network,” en, *Multimedia Tools and Applications*, vol. 77, no. 8, pp. 9909–9924, Apr. 2018, ISSN: 1380-7501, 1573-7721. DOI: 10.1007/s11042-018-5714-1. [Online]. Available: <http://link.springer.com/10.1007/s11042-018-5714-1> (visited on 05/22/2022).
- [15] K. M. Hosny, M. A. Kassem, and M. M. Foad, “Skin Cancer Classification using Deep Learning and Transfer Learning,” in *2018 9th Cairo International Biomedical Engineering Conference (CIBEC)*, Cairo, Egypt: IEEE, Dec. 2018, pp. 90–93, ISBN: 9781538681541. DOI: 10.1109/CIBEC.2018.8641762. [Online]. Available: <https://ieeexplore.ieee.org/document/8641762/> (visited on 05/22/2022).

- [16] P. Tschandl, C. Rosendahl, and H. Kittler, “The HAM10000 dataset, a large collection of multi-source dermatoscopic images of common pigmented skin lesions,” en, *Scientific Data*, vol. 5, no. 1, p. 180 161, Dec. 2018, ISSN: 2052-4463. DOI: 10.1038/sdata.2018.161. [Online]. Available: <http://www.nature.com/articles/sdata2018161> (visited on 05/22/2022).
- [17] Z. Xing, F. Sun, W. He, Z. Wang, X. Song, and F. Zhang, “Downregulation of ubiquitin-specific peptidase 39 suppresses the proliferation and induces the apoptosis of human colorectal cancer cells,” *Oncology Letters*, Feb. 2018, ISSN: 1792-1074, 1792-1082. DOI: 10.3892/ol.2018.8061. [Online]. Available: <http://www.spandidos-publications.com/10.3892/ol.2018.8061> (visited on 05/22/2022).
- [18] S. D. Barman, M. Hasan, and F. Roy, “A Genre-Based Item-Item Collaborative Filtering: Facing the Cold-Start Problem,” en, in *Proceedings of the 2019 8th International Conference on Software and Computer Applications*, Penang Malaysia: ACM, Feb. 2019, pp. 258–262, ISBN: 9781450365734. DOI: 10.1145/3316615.3316732. [Online]. Available: <https://dl.acm.org/doi/10.1145/3316615.3316732> (visited on 05/22/2022).
- [19] S. R. D. and S. A., “Deep Learning Based Skin Lesion Segmentation and Classification of Melanoma Using Support Vector Machine (SVM),” en, *Asian Pacific Journal of Cancer Prevention*, vol. 20, no. 5, pp. 1555–1561, May 2019, ISSN: 2476-762X. DOI: 10.31557/APJCP.2019.20.5.1555. [Online]. Available: [http://journal.waocp.org/article\\_87402.html](http://journal.waocp.org/article_87402.html) (visited on 05/22/2022).
- [20] M. Chen, P. Zhou, D. Wu, L. Hu, M. M. Hassan, and A. Alamri, “AI-Skin: Skin disease recognition based on self-learning and wide data collection through a closed-loop framework,” en, *Information Fusion*, vol. 54, pp. 1–9, Feb. 2020, ISSN: 15662535. DOI: 10.1016/j.inffus.2019.06.005. [Online]. Available: <https://linkinghub.elsevier.com/retrieve/pii/S1566253519300867> (visited on 05/22/2022).
- [21] N. Zhang, Y.-X. Cai, Y.-Y. Wang, Y.-T. Tian, X.-L. Wang, and B. Badami, “Skin cancer diagnosis based on optimized convolutional neural network,” en, *Artificial Intelligence in Medicine*, vol. 102, p. 101 756, Jan. 2020, ISSN: 09333657. DOI: 10.1016/j.artmed.2019.101756. [Online]. Available: <https://linkinghub.elsevier.com/retrieve/pii/S0933365719301460> (visited on 05/22/2022).
- [22] M. Akter, M. S. Hossain, T. U. Ahmed, and K. Andersson, “Mosquito Classification Using Convolutional Neural Network with Data Augmentation,” en, in *Intelligent Computing and Optimization*, P. Vasant, I. Zelinka, and G.-W. Weber, Eds., vol. 1324, Cham: Springer International Publishing, 2021, pp. 865–879, ISBN: 9783030681531 9783030681548. DOI: 10.1007/978-3-030-68154-8\_74. [Online]. Available: [https://link.springer.com/10.1007/978-3-030-68154-8\\_74](https://link.springer.com/10.1007/978-3-030-68154-8_74) (visited on 05/22/2022).
- [23] G. Sambasivam and G. D. Opiyo, “A predictive machine learning application in agriculture: Cassava disease detection and classification with imbalanced dataset using convolutional neural networks,” en, *Egyptian Informatics Journal*, vol. 22, no. 1, pp. 27–34, Mar. 2021, ISSN: 11108665. DOI:



- 10.1016/j.eij.2020.02.007. [Online]. Available: <https://linkinghub.elsevier.com/retrieve/pii/S1110866520301110> (visited on 05/22/2022).
- [24] D. Sarwinda, R. H. Paradisa, A. Bustamam, and P. Anggia, “Deep Learning in Image Classification using Residual Network (ResNet) Variants for Detection of Colorectal Cancer,” en, *Procedia Computer Science*, vol. 179, pp. 423–431, 2021, ISSN: 18770509. DOI: 10.1016/j.procs.2021.01.025. [Online]. Available: <https://linkinghub.elsevier.com/retrieve/pii/S1877050921000284> (visited on 05/22/2022).
- [25] R. L. Siegel, K. D. Miller, H. E. Fuchs, and A. Jemal, “Cancer Statistics, 2021,” en, *CA: A Cancer Journal for Clinicians*, vol. 71, no. 1, pp. 7–33, Jan. 2021, ISSN: 0007-9235, 1542-4863. DOI: 10.3322/caac.21654. [Online]. Available: <https://onlinelibrary.wiley.com/doi/10.3322/caac.21654> (visited on 05/22/2022).
- [26] R. Sujatha, J. M. Chatterjee, N. Jhanjhi, and S. N. Brohi, “Performance of deep learning vs machine learning in plant leaf disease detection,” en, *Microprocessors and Microsystems*, vol. 80, p. 103615, Feb. 2021, ISSN: 01419331. DOI: 10.1016/j.micpro.2020.103615. [Online]. Available: <https://linkinghub.elsevier.com/retrieve/pii/S0141933120307626> (visited on 05/22/2022).
- [27] *VGG Net — Build VGG Net from Scratch with Python*, en, Jun. 2021. [Online]. Available: <https://www.analyticsvidhya.com/blog/2021/06/build-vgg-net-from-scratch-with-python/> (visited on 05/22/2022).
- [28] T. H. Vo, N. T. K. Nguyen, Q. H. Kha, and N. Q. K. Le, “On the road to explainable AI in drug-drug interactions prediction: A systematic review,” en, *Computational and Structural Biotechnology Journal*, vol. 20, pp. 2112–2123, 2022, ISSN: 20010370. DOI: 10.1016/j.csbj.2022.04.021. [Online]. Available: <https://linkinghub.elsevier.com/retrieve/pii/S2001037022001386> (visited on 05/22/2022).
- [29] And, “Automatically early detection of skin cancer: Study based on neural network classification,” Ph.D. dissertation, 2009 International Conference of Soft Computing and Pattern Recognition, IEEE, 2009.
- [30] *Cancer*, en. [Online]. Available: <https://www.who.int/news-room/fact-sheets/detail/cancer> (visited on 05/22/2022).